

UNCLASSIFIED

AD 405 919

DEFENSE DOCUMENTATION CENTER

FOR

SCIENTIFIC AND TECHNICAL INFORMATION

CAMERON STATION, ALEXANDRIA, VIRGINIA



UNCLASSIFIED

NOTICE: When government or other drawings, specifications or other data are used for any purpose other than in connection with a definitely related government procurement operation, the U. S. Government thereby incurs no responsibility, nor any obligation whatsoever; and the fact that the Government may have formulated, furnished, or in any way supplied the said drawings, specifications, or other data is not to be regarded by implication or otherwise as in any manner licensing the holder or any other person or corporation, or conveying any rights or permission to manufacture, use or sell any patented invention that may in any way be related thereto.

405919

ASD-TDR-63-205

RANDOM VIBRATION STUDIES OF COUPLED STRUCTURES IN ELECTRONIC EQUIPMENTS

405 919

TECHNICAL DOCUMENTARY REPORT NO. ASD-TDR-63-205

April 1963

Directorate of Engineering Test
Aeronautical Systems Division
Air Force Systems Command
Wright-Patterson Air Force Base, Ohio

Project No. 1309, Task No. 130904

DDC
JUN 12 1963
TISIA D

(Prepared under Contract No. AF 33(657)-9118
by Bolt Beranek and Newman Inc., Cambridge, Massachusetts;
Richard H. Lyon, Gideon Maidanik, Ewald Eichler, and James J. Coles.)

NOTICES

When Government drawings, specifications, or other data are used for any purpose other than in connection with a definitely related Government procurement operation, the United States Government thereby incurs no responsibility nor any obligation whatsoever; and the fact that the Government may have formulated, furnished, or in any way supplied the said drawings, specifications, or other data, is not to be regarded by implication or otherwise as in any manner licensing the holder or any other person or corporation, or conveying any rights or permission to manufacture, use, or sell any patented invention that may in any way be related thereto.

Qualified requesters may obtain copies of this report from the Armed Services Technical Information Agency, (ASTIA), Arlington Hall Station, Arlington 12, Virginia.

This report has been released to the Office of Technical Services, U.S. Department of Commerce, Washington 25, D.C., in stock quantities for sale to the general public.

Copies of this report should not be returned to the Aeronautical Systems Division unless return is required by security considerations, contractual obligations, or notice on a specific document.

B

FOREWORD

This report has been prepared by Bolt Beranek and Newman Inc., and describes the work completed during the period 15 May 1962 through 15 November 1962 under Contract No. AF 33(657)-9118, entitled, "Dynamic Response and Test Correlation of Electronic Equipment." This work is covered under Project 1309, "Environmental Simulation Investigations for Flight Vehicle Subsystems and Support Equipment," Task 130904, "Development of Simulation Facilities and Test Methods for Induced and Associated Environments."

This program was monitored by the Environmental Division, Directorate of Engineering Test, Aeronautical Systems Division, under the direction of Mr. Robert W. Sevy, Project Engineer.

An earlier report under Contract No. AF 33(616)-7743 covering the period of July 1961 to April 1962 appeared as ASD Technical Documentary Report ASD-TDR-62-614 entitled, "Dynamic Response and Test Correlation of Electronic Equipment."

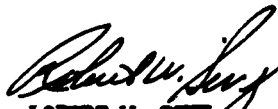
ABSTRACT

The research has centered on two main categories; the replacement of acoustic excitation by direct mechanical excitation of structures and the response of substructures which are tied to a randomly vibrating primary structure. Studies are included on the power transferred to a plate by a shaker, the variation in vibratory response at various positions and frequency bands, and the energy sharing between randomly excited structures which have mechanical connections. Plans for further research are also included.

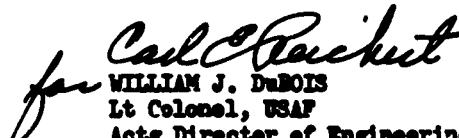
The publication of this report does not constitute approval by the Air Force of the findings or conclusions contained herein. It is published only for the exchange and stimulation of ideas.

REVIEW AND APPROVAL OF ASD TECHNICAL DOCUMENTARY REPORT 63-205


Prepared by:


ROBERT W. SEVI
Project Engineer

Concurred in:


WILLIAM J. DuBOIS
Lt Colonel, USAF
Actg Director of Engineering Test
Deputy for Test and Support

Concurred in:


HUGH S. LIPPMAN
Technical Director
Deputy for Test & Support

Approved by:


ROBERT L. COLLIGAN JR.
Colonel, USAF
Deputy for Test and Support

TABLE OF CONTENTS

<u>Section</u>	<u>Page</u>
RANDOM VIBRATION STUDIES OF COUPLED STRUCTURES IN ELECTRONIC EQUIPMENTS	
	1
A. INTRODUCTION.....	1
B. DESCRIPTION OF OVERALL DIRECTIONS AND PROCEDURES.....	1
C. DESCRIPTION OF SPECIFIC STUDIES AND RESULTS..	3
D. CONCLUSIONS.....	4
 Appendix	
	<u>Page</u>
I POWER FLOW INTO STRUCTURES EXCITED MECHANICALLY...	7
A. INTRODUCTION.....	7
B. EXPERIMENTAL TEST OF EQUATION (1.14).....	11
1. <u>Experimental Apparatus</u>	12
2. <u>Discussion</u>	12
II RESPONSE VARIATIONS IN MULTIMODAL STRUCTURES.....	19
A. INTRODUCTION.....	19
B. THE VARIATION OF RMS RESPONSE IN BANDS OF NOISE FOR MULTIMODAL SYSTEMS.....	20
1. <u>Example</u>	23
C. THE VARIATION OF RMS RESPONSE IN MULTIMODAL STRUCTURES WHEN MODAL OVERLAP IS SMALL.....	24
D. STATISTICAL ESTIMATION OF THE RESPONSE OF A HARMONIC OSCILLATOR ATTACHED TO A FLAT PLATE.....	28
1. <u>Power flow between an oscillator and a flat plate</u>	29

<u>Appendix</u>	<u>Page</u>
2. <u>Relation between power transfer and equilibrium vibration levels</u>	33
3. <u>Confidence levels for estimates of random response</u>	35
III ENERGY SHARING BETWEEN CONNECTED STRUCTURES.....	43
A. INTRODUCTION.....	43
B. BEAM CANTILEVERED TO FLAT PLATE.....	44
1. <u>Theoretical Considerations</u>	44
2. <u>Experimental Considerations and Results</u>	47
C. THE VIBRATION OF CONNECTED PANELS.....	50
1. <u>Introduction</u>	50
2. <u>Flexural Wave Transmission Between Clamped Panels</u>	52
3. <u>Experimental Study</u>	56
4. <u>Vibratory Response of Cantilevered Panel</u>	57
D. REDUCTION OF BEAM-PLATE COUPLING BY NOTCHING BEAM.....	57

LIST OF FIGURES

<u>Figure</u>		<u>Page</u>
1.1	Acceleration Level Difference Between Driving Point and Reverberant Field for 3' x 4' Panel.....	14
1.2	Acceleration Level Difference Between Driving Point and Reverberant Field for 3' x 4' Panel.....	15
1.3	Acceleration Level Difference Between Driving Point and Reverberant Field for 3' x 4' Panel.....	16
1.4	Panel Excitation System.....	17
1.5	Vibration Detection System.....	18
2.1	Graph of $10 \log f(N)$	39
2.2	Diagram of Plate with Attached Oscillator....	40
2.3	Oscillator Sketch, Mechanical Diagram, and Mobility Analog Equivalent Circuit.....	41
2.4	Safety Factor in Estimation Required to Achieve Given Confidence Level.....	42
3.1	Analog Circuit for the Moment at the Beam-Plate Interface.....	60
3.2	Schematic Diagram of Beam-Plate System.....	61
3.3	Direct and Indirect Measurements of Response Ratios Without Applied Damping.....	62
3.4	Direct and Indirect Measurements of Response Ratios with Applied Damping.....	63
3.5	Experimental Flow Diagram for Direct Measurement of S_y/S_p^a	64

<u>Figure</u>		<u>Page</u>
3.6	Plate Geometry.....	65
3.7	Plate Boundary Conditions.....	65
3.8	Loss Factors and Absorption Coefficient of 0.032" Glued Aluminum Plate.....	66
3.9	Loss Factors and Absorption Coefficient of 0.031" Welded Steel Plate.....	67
3.10	Loss Factors and Absorption Coefficient of 0.057" Welded Steel Plate.....	68
3.11	Plate-Beam System Showing The Cut Made to Reduce the Coupling.....	69
3.12	The Response of a Beam Cantilevered to Flat Plate.....	70
3.13	Relative Vibration Levels of Connected Reverberant Plates.....	71
3.14	Relative Vibration Levels of Connected Reverberant Plates (Plate 1 Lightly Damped)..	72

RANDOM VIBRATION STUDIES OF COUPLED STRUCTURES IN ELECTRONIC EQUIPMENTS

A. INTRODUCTION

The advent of rocketry telemetry and control requires electronic packages and components which must withstand severe acoustic and vibrational environments. One step in the design of these packages is the estimation of acoustic and vibrational environments. Another is concerned with vibration and sound reduction through the design of vibration and noise control treatments. Finally, there is a proof testing requirement which leads one to seek methods of establishing the expected package or component environment in a laboratory situation.

These requirements all dictate a need for better understanding of the laws governing energy transfer between randomly vibrating systems. In the following sections of this report we shall describe our efforts to improve this understanding. In Section B, we outline the general problem of predicting and simulating response of complicated structures. We then define certain subareas and tasks which one must study as part of the more general problem. In Section C we describe our studies and results thus far on some of these tasks. Finally, in Section D, we indicate some of the additional tasks to be performed during the remaining parts of this contract.

B. DESCRIPTION OF OVERALL DIRECTIONS AND PROCEDURES

An electronic package in a random noise environment receives its energy by two primary paths, direct acoustic excitation and mechanical vibration through its attachment points. We will normally assume that the power from these two sources is additive. Correlation effects which would cause departures from additivity, are possible since the surrounding structure generates sound about the package. The vibrations of the base structure may therefore be correlated with the sound field. The difference in propagation times for sound and mechanical energy and the differences in excitation efficiencies may be expected, however, to minimize the effect of any correlated behavior.

Manuscript released by the authors 15 November 1962 for publication as an ASD Technical Documentary Report.

If one computed the power absorbed by the package from the sound field and through its mounting points, then a proof test of the design can be made by the direct application of this power. To apply this power with a sound field however requires very expensive sound sources. It has been suggested that one might be able to substitute direct mechanical excitation instead.

The power fed into a panel-frame structure by a random noise sound field has been studied at BBN both theoretically and experimentally (Refs. 1-3). The approach is statistical in its description of the random noise process, and it is also statistical in its description of the structure. Rather than analyze a structure with precise dimensions, mounting conditions, damping treatments, etc., one describes the structure by an average modal density, total area and edge length of panels, loss factor, etc. This allows one to apply the results to a wider class of structures, but one must also be concerned with how variations in response will arise from one structure to another due to the variations in these statistical measures. These same considerations will arise when we discuss how energy is transferred between structural attachments.

In this present program, we have asked the following specific questions:

- a) What are the laws of energy transfer between connected structures? The answer to this tells us how much energy will get to a package through its mountings and further, the amount of energy which travels to internal panels of the package.
- b) Since our answers to (a) are essentially average values of statistical results, what variations may we expect as we go from one structure to another, or from one part of the frequency spectrum to another, or from one position on the structure to another? A knowledge of the variations will allow us to set confidence levels on any range of estimates we may wish to consider.
- c) If we wish to supply mechanical power to the package, not through its normal environmental condition, but by direct application of high frequency shakers, can we develop reliable estimates of input power? Also, can we develop techniques for measuring the input mechanical power directly?
- d) Finally, can we use these theoretical results to actually predict response of a simple package-sub-panel system in a noise and vibration environment? If the answer to this is "yes," then our confidence in the theoretical-experimental procedures referred to above is augmented.

C. DESCRIPTION OF SPECIFIC STUDIES AND RESULTS

We will now describe specific studies which we have launched to answer the questions posed in the preceding section. These studies are not complete, but we feel that a good beginning has been made. The studies themselves appear as a series of Appendices to the report. Here we shall merely review their motivation and discuss the main results very briefly.

I. Power Flow Into Structures Excited Mechanically

A shaker may be mounted to a structure by a stud attachment. Normally this stud is sufficiently small compared to a wavelength of bending waves and the structural dimensions that it may be considered a point force. The power this source feeds into the structure, therefore, depends on the point impedance at the position of application. This impedance is usually a highly fluctuating function of frequency for finite structures, but if one is concerned with average response over a band of frequencies, then the infinite system input impedance may theoretically be used.

The study of a shaker driven plate in Appendix I is an attempt to test the assumption that the average power fed into the plate in third octave bands can be calculated on the basis of the known force from the shaker and the input resistance of the infinite plate. The early conclusion seems to be that this is possible if one will accept an uncertainty of the order of 3 db.

II. Response Variations in Multimodal Structures

Most of the studies of sound to vibration and vibration to vibration interaction generate estimates of average energy levels or power flow in frequency bands. These estimates are more nearly exact as one averages over more modes of response, positions of observation and types of structures. Some concern has arisen about the confidence one can have in these average values if one is dealing with only a few modes, or observation points, or structures. To generate directly procedures for evaluating confidence levels for the estimates, we have initiated a set of studies on the variations in response for various cases.

In Appendix II these variation studies are reported. We have studied the variations in response at one position when the structure is point excited at a second position (Sections B and C) and the response of a simple oscillator when it is attached to the plate (Section D). The first study is appropriate to expected variations in estimating the vibration of the plate itself while the second is concerned with variations in substructure response--in particular in regions of low modal density.

III. Energy Sharing Between Connected Structures

The power flow between structures and their vibration levels are studied by considering each structure as a collection of modes. These modes are coupled by the connection of the structures. The evaluation of this coupling requires detailed calculation of input impedances of various types for infinite systems just as the sound-structure problem requires computation of radiation resistance for various configurations. Our work on connected structures, therefore, has involved the computation of these impedances for cantilevered beams attached to plates and for plates joined together either by continuous welds or studs. It has also involved experiments on the systems analyzed theoretically to establish whether in fact one can get agreement with theoretical estimates.

The details of the work in this area are reported in Appendix III. In general, our results for vibration levels in the cantilevered beam and the welded plate are quite encouraging.

D. CONCLUSIONS

Power flow into structures excited mechanically. In this area we are developing techniques for measuring the force velocity product so that input power may be measured directly for pure tones or bands of noise. This means that experimentally we do not have to rely on computation of input impedances or structures with the attendant uncertainty in parameter values.

Variance analysis of multimodal structures. We now feel that variance and confidence analysis has been sufficiently well established as a theoretical tool. We do not, therefore, plan further theoretical studies in developing the method. It will instead become a part of the power flow and energy sharing studies and be used and tested in the experimental aspects of that work.

Energy sharing between connected structures. We should like to consider at least two systems which have not been studied experimentally at this time. One is a study of plates connected by stud mountings, a type of connection which is very common in real packages. The second is the response of a single oscillator attached to a plate. This is essentially a test of some of the variance studies reported in Appendix II. In addition to these, some additional theoretical studies of plate-beam decoupling by notching of the beam would be in order.

Environmental estimates and simulation for package-panel structure. We plan to take a box with an internal panel and place it in a sound field, measuring the resulting vibrational levels. With a knowledge of the damping, we expect to correlate these levels with the radiation resistance of the structure. This part of the experiment is essentially a repeat of an earlier study (Ref. 3). Then we will apply some input power with a shaker and again measure vibration levels, with special attention to seeing whether the acoustic response can be simulated in this way. Comparisons of internal panel response with package wall response should afford a reasonable test of our energy sharing calculations.

NOTES AND REFERENCES

1. R. H. Lyon and G. Maidanik, "Power flow between linearly coupled oscillators," J. Acoust. Soc. Am. 34, 5, 623, May, 1962.
2. G. Maidanik, "Response of ribbed panels to reverberant acoustic fields," J. Acoust. Soc. Am. 34, 6, 809, June, 1962.
3. D. U. Noiseux, J. J. Coles, N. Doelling, R. H. Lyon, "Response of electronics to intense sound fields," Report No. 871, Bolt Beranek and Newman Inc., Cambridge, Massachusetts, July, 1961, Section III.

APPENDIX I

POWER FLOW INTO STRUCTURES EXCITED MECHANICALLY

A. INTRODUCTION

In this appendix we consider the injection of mechanical power into a structure by an electromechanical shaker. The first step is the determination of the coupling between the mechanical shaker (or a system of shakers) and the structure we wish to test. We propose to substitute this mechanical excitation for the acoustic power supplied to the structure by a sound field.

The power absorbed from a reverberant sound field of mean square pressure $\overline{p^2}$ is given by (Ref. 1)

$$P_{in} = \frac{2\pi^2 n_s(\omega) c^2 A_p}{M_s \omega^2} \sigma_{rad} \overline{p^2} \quad (1.1)$$

where

- M_s is the mass of the structure,
- ω is the center (radian) frequency of excitation,
- c is the speed of sound in air,
- A_p is the irradiated area of the structure,
- $n_s(\omega)$ is the average modal density of the structure,
- σ_{rad} is the radiation efficiency of the structure averaged over A_p and the frequency band of the excitation.

It is this power that we want to supply by the shaker system. The power which a shaker can feed to the structure will depend on the real part of the mechanical impedance presented to it. We may define the mechanical impedance

$$Z_{in} = R_{in} - i X_{in} \quad (1.2)$$

The power input in terms of the mean square acceleration at the shaker $\overline{a_d^2}$ (in the absence of reverberation) is

$$P_{in} = \frac{\overline{a_d^2} R_{in}}{\omega^2} \quad (1.3)$$

where we have assumed that R_{in} is a fairly smooth function of frequency. In the initial stages of the computations we shall use an impedance which is averaged over several modes of vibration. If we equate Equation (1.1) with Equation (1.3) we obtain for the mean square pressure

$$\overline{p^2} = \overline{a_d^2} \frac{R_{in} M_s}{2\pi^2 n_s(\omega) c_p^2 A_p \sigma_{rad}} \quad (1.4)$$

We shall be studying the mechanical-acoustical equivalence in the case of panels. For a panel of thickness, h , material density, ρ_p , and longitudinal velocity, c_ℓ , the modal density is given by (Ref. 1)

$$n_s(\omega) = \frac{\sqrt{3} A_s}{2\pi h c_\ell} \quad (1.5)$$

where A_s is the panel surface area (one side).

The expression for the impedance for an infinite panel is

$$R_{in} = Z_1 = \frac{4}{\sqrt{3}} \rho_p c_\ell h^2 \quad (1.6)$$

For a finite panel the same equation is obtained when the input impedance is averaged over several modes. Our assumption is that in a narrow frequency band (e.g., third octave) several modes of the panel will be excited.

The radiation efficiency for a baffled* panel is (Ref. 2)

$$\sigma_{\text{rad}} \simeq \frac{\pi P_r h}{\sqrt{3} A_p} \frac{c_l}{c} (f/f_p)^{1/2}, \quad f < \frac{1}{2} f_p \quad (1.7)$$

where P_r is the perimeter of the panel and f_p is the acoustic coincidence frequency. The expression for σ_{rad} is valid if the sound field and the vibrational field of the structure are reverberant and the dimensions of the panel are greater than one-third of an acoustic wavelength. For other frequency conditions, the expression is somewhat more complicated, (Ref. 2). Substituting Equations (1.5), (1.6), and (1.7) in Equation (1.4), we obtain

$$\overline{p^2} = \overline{a_d^2} \frac{\rho_p^2 h^2}{\sqrt{3}} \frac{c_l}{c} \frac{h}{P_r} \left(\frac{f_p}{f} \right)^{1/2} \quad (1.8)$$

For a Goodmans shaker (Goodmans Industries, Ltd., Model 390A) the limiting rms acceleration when unloaded is about 100 g's. If the shaker is attached to a point of a panel whose point impedance is R_{1n} the mean square acceleration at the point is

$$\overline{a_d^2} = \overline{a_o^2} \frac{(um_c)^2}{(um_c)^2 + R_{1n}^2} \quad (1.9)$$

where um_c is the mass reactance of the moving coil assembly. This is the mean square acceleration which we use in defining P_{1n} in Equation (1.3). For a panel with $h = 3.16 \times 10^{-1}$ cm, $\rho_p = 2.7$ gm/cm³, $c_l = 5 \times 10^5$ cm/sec, and $P_r = 610$ cm, the maximum available equivalent sound pressure level in db is about

* In this section we are interested in determining the power fed into a structure by mechanical excitation. For the specific case of a panel excited by mechanical means, whether the panel is baffled or not is not important, as long as the radiation damping is smaller than the mechanical damping. However when one wants to study experimentally the equivalence between the acoustical and mechanical power supplied to the structure, whether the panel is baffled or unbaffled becomes essential. For an unbaffled panel the radiation efficiency σ_{rad} is much lower than the one given in Eq. (1.7).

$$142 + 5 \log_{10} (f_p/f) + 10 \log_{10} \left\{ \frac{(am_c)^2}{(am_c)^2 + R_{1n}^2} \right\} \quad (1.10)$$

For the panel under consideration $f_p \approx 4$ kc (aluminum panel) and $R_{1n} = 3.12 \times 10^5$ gm/sec. The mass of the moving coil assembly of the Goodmans shaker (Model 390A) is about 72 gm. Thus, the maximum equivalent sound pressure capability of this Goodmans shaker with respect to the given panel is at 100 cps about 138 db and at 1 kc about 148 db.

When an accelerometer is placed at the point to which the shaker is connected the acceleration measured at this point may be influenced by the reverberant field of the panel. The exact expression is

$$\overline{a_s^2} = \overline{a_d^2} + \overline{a_r^2} \frac{R_{1n}^2}{R_{1n}^2 + \omega^2 m_c^2} \quad (1.11)$$

where $\overline{a_s^2}$ is the mean square acceleration indicated by the accelerometer and $\overline{a_r^2}$ is the mean square acceleration of the reverberant vibrational field.

The power supplied by the shaker must be equal to the power dissipated in the system. This equality enables us to test our formalism experimentally. The damping in the panel-shaker system may be expressed in terms of a loss factor

$$\eta = \frac{13.8}{\omega T_p} \quad (1.12)$$

The dissipated power is

$$P_{diss} = \overline{a_r^2} (M_s \eta / \omega) \quad (1.13)$$

where T_p is the reverberation time of the system. Equating Equation (1.3) to Equation (1.13), and making use of Equation (1.11), so that the mean square accelerations involved are measurable quantities, we obtain

$$\overline{a_s^2} = \overline{a_r^2} \left\{ \frac{M_s \eta \omega}{R_{in}} + \frac{R_{in}^2}{R_{in}^2 + \omega^2 m_c^2} \right\} \quad (1.14)$$

Thus, measurements of $\overline{a_s^2}/\overline{a_r^2}$ will give us the experimental value of the bracketed quantity in Equation (1.14). On the other hand, measurements of η [by reverberation time measurements and the use of Equation (1.12)], the use of the given value of $m_c = 72$ gm in our case) and the theoretical value of R_{in} as given by Equation (1.6) will enable us to calculate the bracketed factor in Equation (1.14) by an independent method. Comparison between these two determinations should give us a cross check for our theory. It may be in order to summarize at this point the fundamental assumptions that we made and that therefore must be satisfied for fair comparison to be possible.

- a) The vibrational field of the panel is reverberant in the sense that all or most of the modes in a given frequency band (e.g., third octave) are participating in the vibration and that the vibrational field is diffuse. An experimental test for the reverberant field is that the vibrational level of the panel when excited by noise filtered through a given frequency band will be essentially independent of position.
- b) The point impedance of the panel approximates that of the point impedance of an infinite panel. Theoretically, if (a) is satisfied, so is (b).

B. EXPERIMENTAL TEST OF EQUATION (1.14)

An experimental arrangement has been designed and constructed to test Equation (1.14) which is derived in Section A. The difference in acceleration levels at the driving point and a selected number of points on the panel were measured. The reverberation time of the panel-shaker system was also determined experimentally and the bracketed expression in Equation (1.14) was calculated in accordance with the procedure indicated at the end of Section A. The latter calculations were then compared with the measured values of the ratio $\overline{a_s^2}/\overline{a_r^2}$. The results for three different cases, undamped, lightly damped and heavily damped panels, are given in graphical form in Figures 1.1, 1.2, and 1.3.

1. Experimental Apparatus

An aluminum panel 3' x 4' x 0.129" was suspended from the ceiling on nylon cords from two corners. Otherwise it was unrestrained. A vibration shaker was arranged to excite the panel at a point. The location of the driving point was chosen away from the edge of the panel. The attaching hardware was devised to provide only transverse motion and minimize applied torque and damping at the driving point.

The excitation was in third octave bands of random noise. The output of the accelerometer attached at the driving point was compared successively with the output of the accelerometer attached at several points on the panel surface (see Figures 1.1, 1.2, and 1.3 for the exact locations which are indicated by circled numbers). The output of the accelerometers was recorded on a graphic level recorder. The flow diagram of the experimental arrangement is shown in Figure 1.4.

The reverberation time was determined using a graphic level recorder and the reverberation-time apparatus described in reference 4 of Appendix III. A pulse technique was used for the reverberation time measurements; the panel was tapped with a metallic hammer at various positions on the panel and its decay was measured by measuring the filtered (third octave band) output of an accelerometer. The flow diagram for the experimental arrangement is shown in Figure 1.5.

2. Discussion

Although there is a general correlation between the results of the two methods of determining the factor of proportionality relating \bar{a}_s^2 to \bar{a}_r^2 , in detail the agreement is not completely satisfactory. Further improvement in the theoretical approach may therefore be necessary. It should be pointed out that for the undamped and lightly damped case the vibrational field could be assumed reverberant. The measurements taken at the three positions on the panel did not vary by more than 2 db. In the case of the heavily damped panel the variation in level between the four positions, where measurements were taken, in several instances exceeded 6 db. These large differences in level were not confined to any particular frequency range. Moreover, the measurements of reverberation time for the heavily damped panel at frequencies above 3 kc are not very reliable; they were taken at the limit of the range of the instrument used. The reverberation times above 3 kc were of the order of 10^{-2} sec. in this case. We note here that some of the theoretical results from Section B in Appendix II anticipate the higher fluctuations in response for the very heavily damped panel.

REFERENCES FOR APPENDIX I

1. R. H. Lyon and G. Maidanik, "Power flow between linearly coupled oscillators," J. Acoust. Soc. Am. 34, 5, 623 May, 1962.
2. G. Maidanik, "Response of ribbed panels to reverberant sound fields," J. Acoust. Soc. Am. 34, 6, 809, June, 1962.

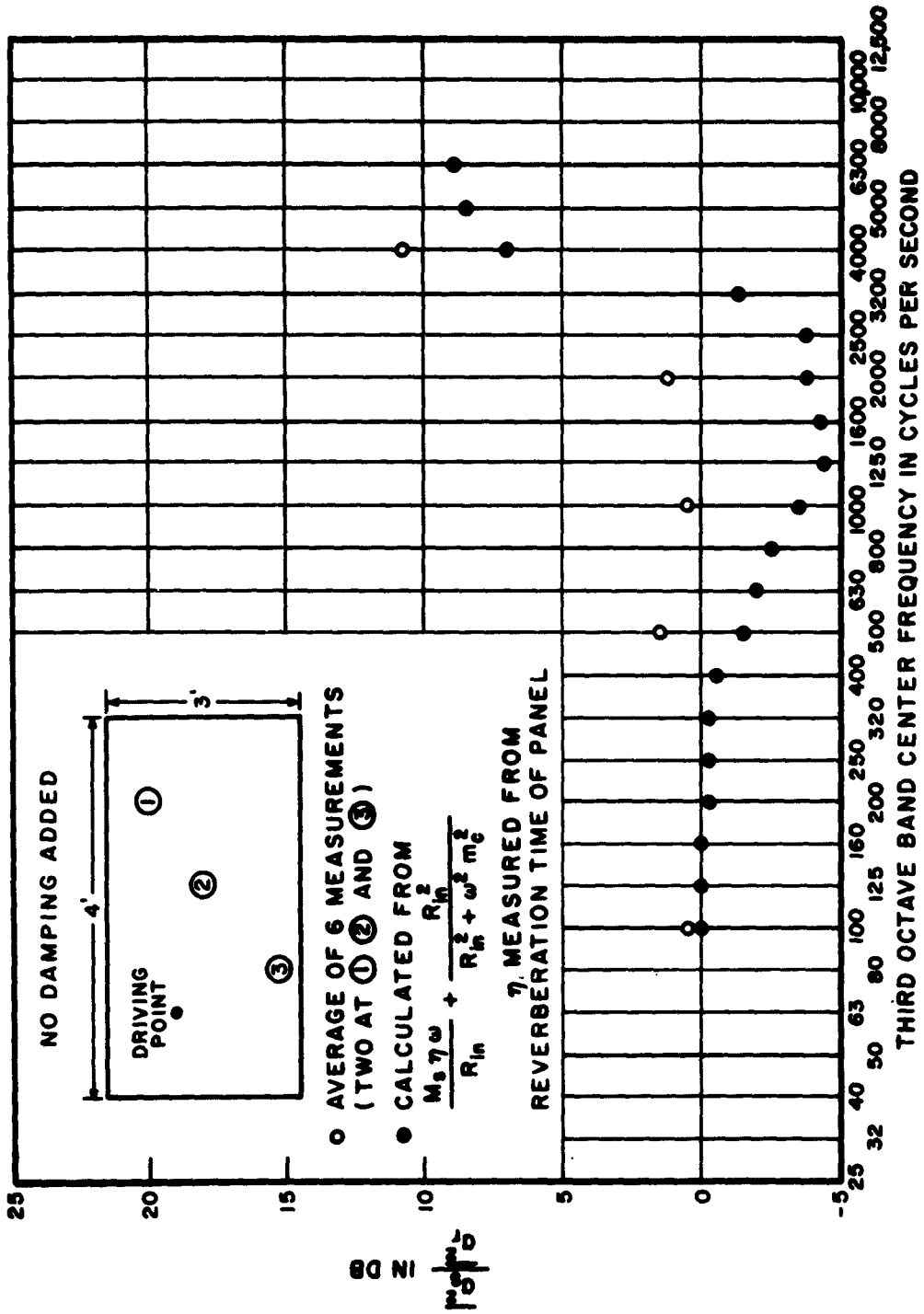


FIG. 1.1 ACCELERATION LEVEL DIFFERENCE BETWEEN DRIVING POINT AND REVERBERANT FIELD FOR 3' x 4' PANEL

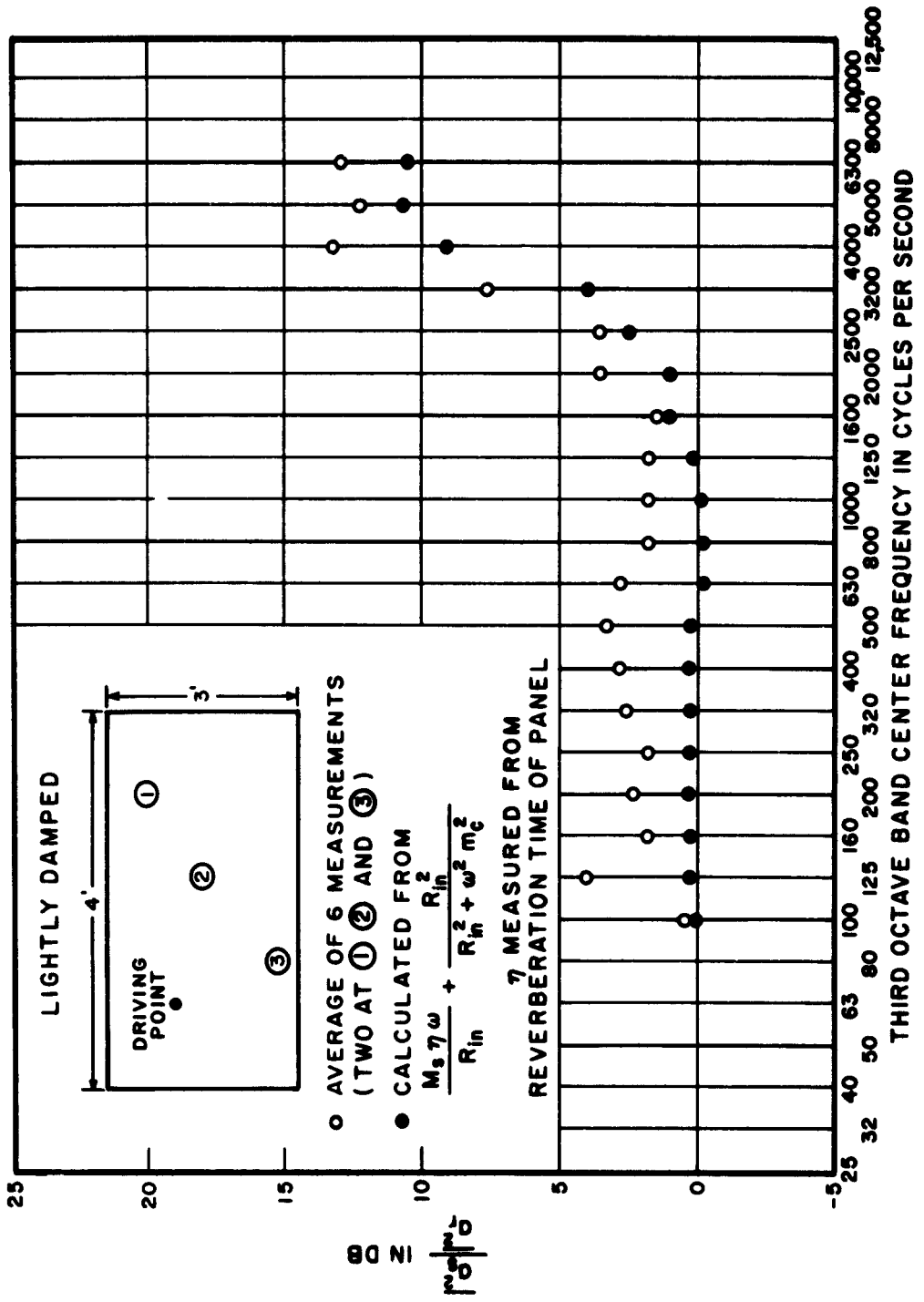


FIG.1.2 ACCELERATION LEVEL DIFFERENCE BETWEEN DRIVING POINT AND REVERBERANT FIELD FOR 3' x 4' PANEL

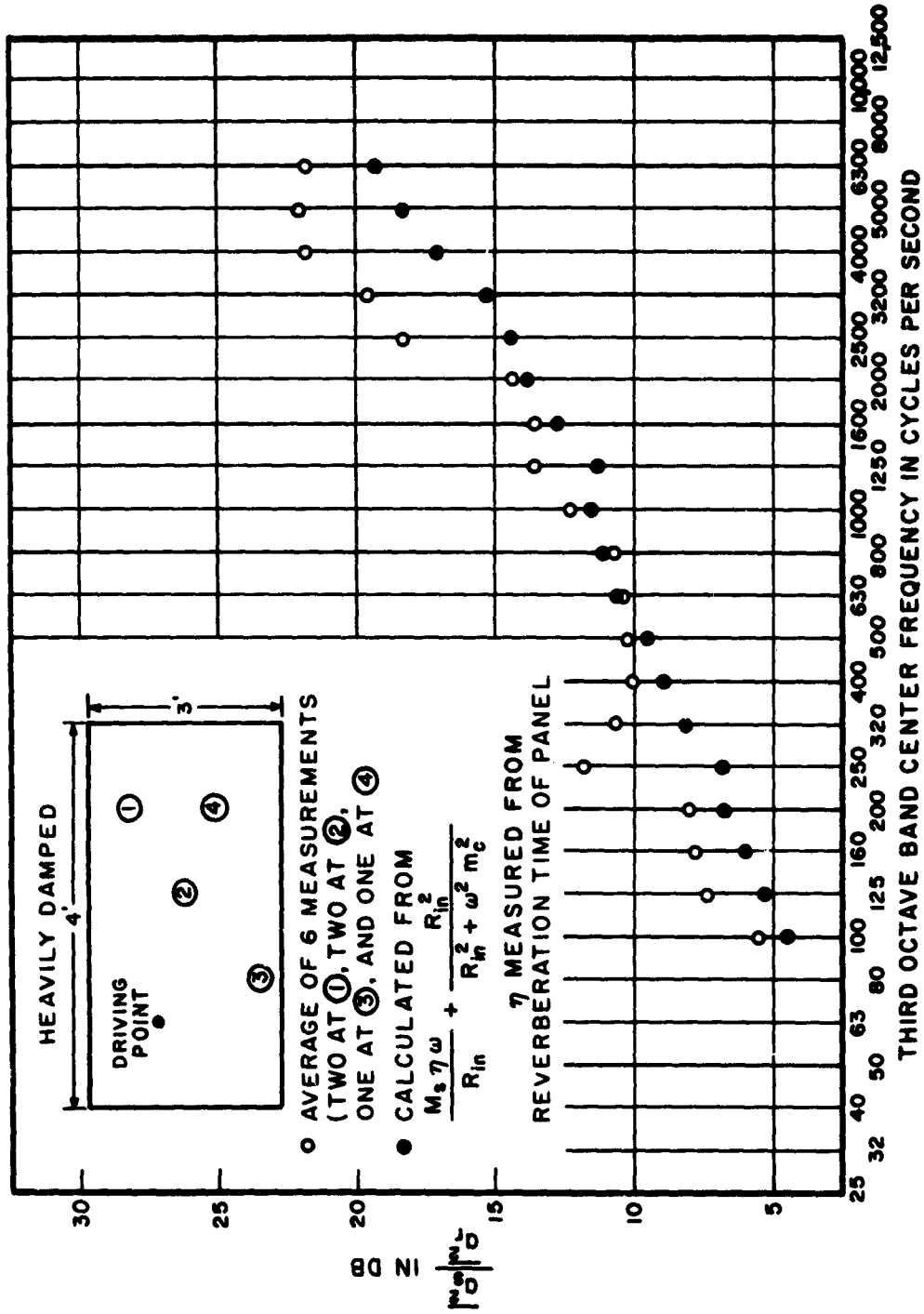


FIG. 1.3 ACCELERATION LEVEL DIFFERENCE BETWEEN DRIVING POINT AND REVERBERANT FIELD FOR 3' x 4' PANEL

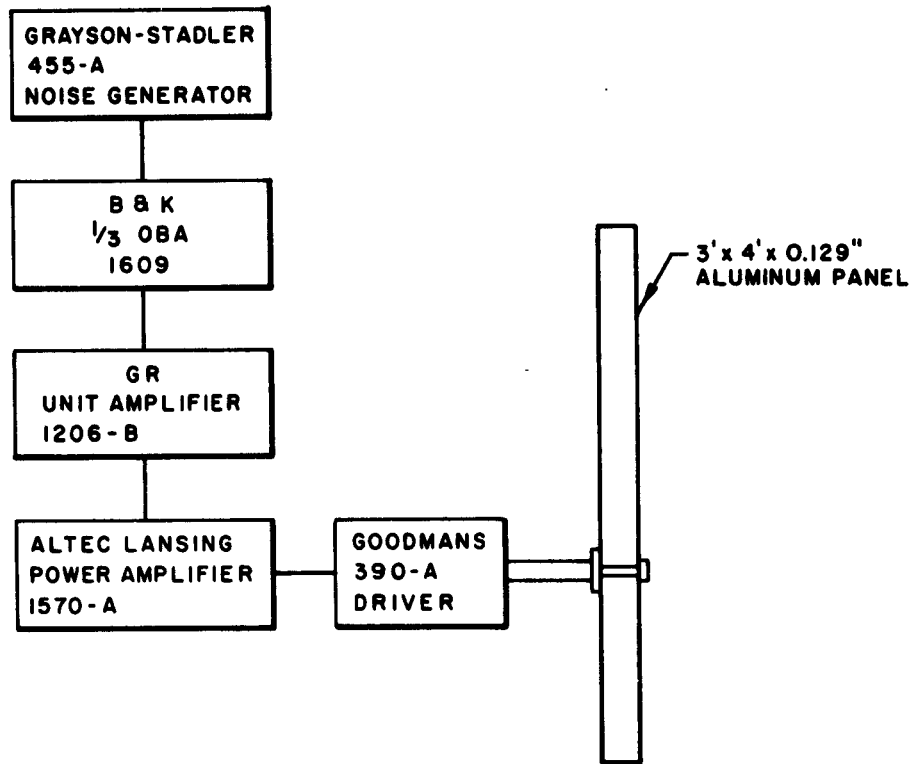


FIG.1.4 PANEL EXCITATION SYSTEM

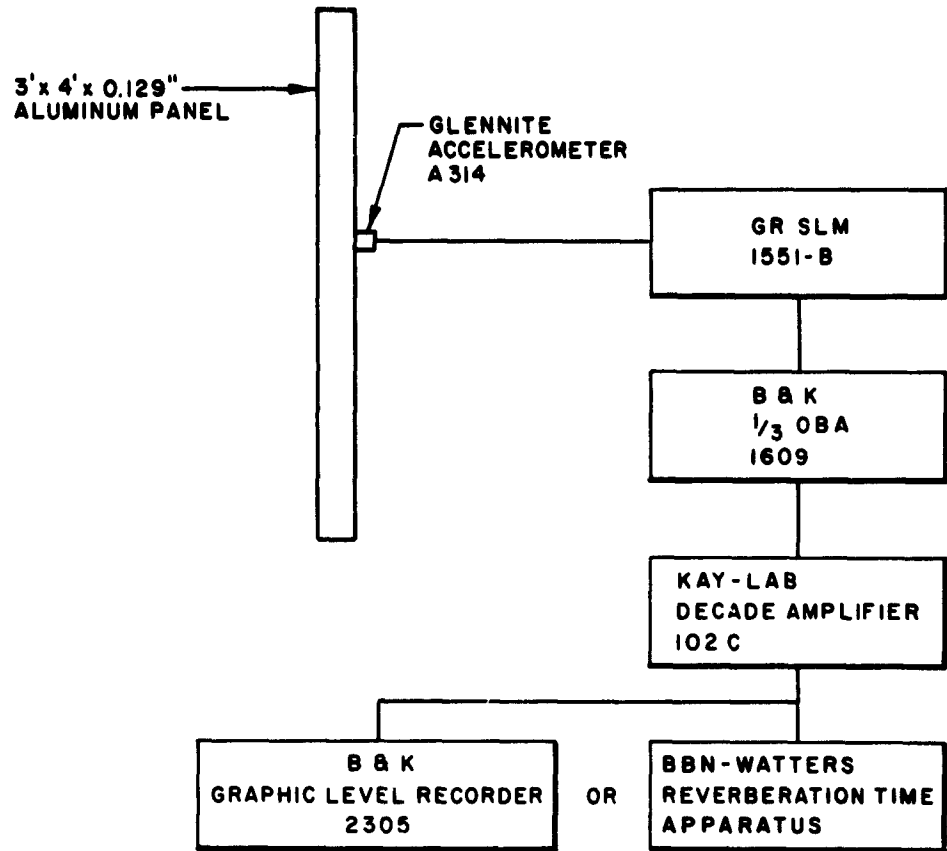


FIG. I.5 VIBRATION DETECTION SYSTEM

APPENDIX II

RESPONSE VARIATIONS IN MULTIMODAL STRUCTURES

A. INTRODUCTION

In the past few years, the response of complex structures made up of panels, supporting members, struts, etc., to random noise fields has received a good deal of attention at Bolt Beranek and Newman Inc., and other research centers. At BEN we have described not only the temporal response in a statistical way, but the structure itself as well (Ref. 1). Thus, a structure is defined by its distribution of modal resonances in frequency, average lengths of beams, areas of panels, etc. The results of this procedure have been encouraging in their ability to predict certain average characteristics of response when many modes of vibration are involved.

For small structures in the lower frequency ranges, one may not always have a very large number of modes contributing to the response. One effect of this will be to cause fluctuations about the average value in the observed response from one frequency band to the next (Ref. 2), which we shall refer to as frequency variation. Also, there will be variation in response as one moves from one measuring point to another on the structure. This spatial variation will be important as an additional source of variation in the comparison of theoretically computed average values and experimentally measured values. Also, one should note that we are not concerned here with the temporal fluctuations of the signal as a random process in time. We assume that sufficient averaging time is used for the measurement so that variations due to this effect are negligible.

It is ambiguous to speak merely of "the variation" since the response variable we have in mind has not been specified. Analytically, the variation in (time) average response (velocity, acceleration, strain, etc.) is convenient to deal with. Experimentally, response is read out and plotted in logarithmic units, and the variation visible on the experimental plot is in decibels, not so many g's (for example). Unfortunately, a great deal must be known about the response in order to get its logarithmic variation. If, for example, we know the standard deviation of the acceleration, we cannot go from this value to a standard deviation for the response in decibels. Indeed, the entire probability density for the response would be required to evaluate the logarithmic variation. In some cases we shall find it possible to make this computation, in others we will have to be satisfied with the variation in the dynamical variable itself.

B. THE VARIATION OF RMS RESPONSE IN BANDS OF NOISE FOR MULTIMODAL SYSTEMS

We wish to find the variation in mean square response (velocity, say) for a structure, which has a pure tone mean square response* given by $W(\omega)$, when that structure is excited by a band of noise of width Δ centered about the frequency ω . The response for band excitation of bandwidth Δ and spectral density $\frac{1}{\Delta}$ is

$$V(\omega_0) = \frac{1}{\Delta} \int_{\omega_0 - \Delta/2}^{\omega_0 + \Delta/2} W(\omega) d\omega. \quad (2.1)$$

Let the average response $\bar{W}(\omega)$, be the response $W(\omega)$ averaged over similar structures or over different positions on the same structure. The band response, to excitation of bandwidth Δ and spectral density $\frac{1}{\Delta}$, of the average response $\bar{W}(\omega)$ is

$$m_V(\omega_0) = \bar{V}(\omega_0) = \frac{1}{\Delta} \int_{\omega_0 - \Delta/2}^{\omega_0 + \Delta/2} \bar{W}(\omega) d\omega = m_W(\omega_0) \quad (2.2)$$

provided $\bar{W}(\omega)$ varies only slightly over the bandwidth of excitation due to changes in modal density or damping.

One measure of the variation in response for band excitation is the standard deviation σ_V of V which is found from the variance

$$\begin{aligned} \sigma_V^2 &= \overline{V^2} - \bar{V}^2 \\ &= \sigma_W^2 \frac{1}{\Delta^2} \iint d\omega_1 d\omega_2 \phi_W(\omega_1 - \omega_2) \end{aligned} \quad (2.3)$$

* "response" in this section means "mean square response in time" in all cases.

where

$$\sigma_w^2 = \overline{w^2} - m_w^2$$

is the variance of the sinusoidal response,

and

$$\phi_w(\omega_1 - \omega_2) = \frac{\overline{w(\omega_1)w(\omega_2)} - m_w^2}{\sigma_w^2} \quad (2.4)$$

In the case of multimodal systems with a high degree of modal overlap (a situation appropriate to rooms but not as common in complex structures) Schroeder has shown that the correlation function for pure tone response (Ref. 3) is of the form

$$\phi_w(\xi) = \frac{4\alpha^2}{\xi^2 + 4\alpha^2} \quad (2.5)$$

where α is the modal decay constant, related to the structural loss factor η by

$$\eta = 2\alpha/\omega \quad (2.6)$$

Also, Schroeder has shown (Ref. 4) that the distribution of w is given by the exponential density

$$\psi(w) = \frac{1}{m_w} e^{-w/m_w} \quad (w > 0) \quad (2.7)$$

which has a variance

$$\sigma_w^2 = 2m_w^2 \quad (2.8)$$

If we place Equation (2.5) in Equation (2.3) and transform to variables

$$\left. \begin{aligned}
 \xi &= \omega_1 - \omega_2 \\
 \eta &= \omega_1 + \omega_2 \\
 d\xi \, d\eta &= 2 \, d\omega_1 \, d\omega_2
 \end{aligned} \right\} \quad (2.9)$$

then the integration becomes

$$\begin{aligned}
 \sigma_v^2 &= \frac{2\sigma_w^2}{\Delta^2} \int_0^\Delta d\eta \int_0^{\Delta-\eta} d\xi \phi_w(\xi) \\
 &= \frac{4\alpha}{\Delta^2} \sigma_w^2 \int_0^\Delta d\eta \tan^{-1} \frac{\Delta-\eta}{2\alpha} \\
 &= \frac{1}{N} \sigma_w^2 \left[\frac{2}{\pi} \tan^{-1} \pi N - \frac{1}{\pi^2 N} \ln(1 + \pi^2 N^2) \right] \\
 &= \frac{1}{N} \sigma_w^2 f(N)
 \end{aligned} \quad (2.10)$$

where $N = \Delta/2\alpha$ is the ratio of excitation bandwidth to the effective bandwidth of the resonant modes. As $N \rightarrow \infty$, the term in the brackets which is plotted in Figure 2.1 goes to unity and one has a result reminiscent of a central limit type of convergence of V on its mean value.

We note that the ratio between band variance σ_v and pure tone variance σ_w depends only on the ratio of exciting bandwidth to modal bandwidth only; there is no dependence on modal spacing because of the model used. This may be because we have assumed a high degree of modal overlap in using Schroeder's formulas, which means that the modal bandwidth 2α is large compared to the average spacing between modes. In Section C of this Appendix, we extend these results to the region of low modal density which is a more appropriate regime for structures.

We note from the result Equation (2.10) that the fluctuation increases as the damping α increases. Our intuitive feeling, however, is that the response should "smooth out" as damping is added. This is true in the low mode overlap region to be studied. For high modal overlap however, the rapidity of fluctuation in the pure tone response decreases with increased damping, while the variation in response remains more or less constant. Thus if we average this response over a fixed band of frequencies, we average over fewer variations when the damping is higher, and we may expect to see greater variation in the average.

The variance of band response can be expressed in terms of its mean

$$\begin{aligned}\sigma_v^2 &= \frac{1}{N} \sigma_w^2 f(N) = \frac{2}{N} m_w^2 f(N) \\ &= \frac{2}{N} f(N) m_v^2 ,\end{aligned}$$

or,

$$\sigma = \sqrt{\frac{2}{N} f(N)} m_v ,$$

where we have used Equation (2.2).

Thus, for the average $\overline{v_p^2}$ of a set of measured responses,

$$\sigma_{v^2} = \sqrt{\frac{2}{N} f(N)} \overline{v_p^2} . \quad (2.11)$$

1. Example

A large panel has a loss factor $\eta = 10^{-2}$ and an average modal separation of 4 cps. A resonant filter is equivalent to a rectangular filter of bandwidth $\pi\eta f$. At 1 kc, this effective modal bandwidth is 31.4 cps. Thus, on the average there is an overlap of 7 or 8 modes which is probably sufficient to meet Schroeder's criterion. We can ask what the standard deviation would be in the third octave band centered on 1 kc. In this case, the bandwidth of excitation is 260 cps and

$$N = \frac{\Delta}{\pi\eta f} = 8.28 .$$

From Figure 2.1, $f(8.28) = 0.9$ and

$$\sigma_{v^2} = \sqrt{\frac{2}{8}} \overline{v_p^2} = \frac{1}{2} \overline{v_p^2} .$$

Thus, the standard deviation in response will be about 3 db from the average. By repeating the measurement at several points on the structure, this uncertainty may of course be reduced. If we take $\eta = 2 \times 10^{-3}$, then $\pi\eta f = 6.3$ cps, and $N = 41.4$. Thus

$$\sigma_{v^2} = \overline{v_p^2} / \sqrt{20} = 0.224 \overline{v_p^2}$$

which is only about 1 db variation about the mean. Of course, we are now probably violating the condition of strong modal overlap, but the point can be made that damping increases the fluctuation in this region. This observation appears to be supported by some of our preliminary experiments (see Appendix I).

C. THE VARIATION OF RMS RESPONSE IN MULTIMODAL STRUCTURES WHEN MODAL OVERLAP IS SMALL

In Section B we showed that the band response of the structure was related to the pure tone response in a very simple manner. In particular, the variance of band and pure tone response were related as indicated in Equation (2.3). This relation is unaffected by any assumptions of modal density, damping, etc. We may therefore use it as a starting point in our present analysis.

Again calling $W(\omega)$ the mean square pure tone response we require its autocorrelation function $\Phi_W(\xi)$. This is found by first considering the response amplitude

$$y(\omega) = \sum_m b_m g_m(\omega) \tag{3.1}$$

where b_m is an excitation coefficient and $g_m(\omega)$ is a harmonic oscillator (modal) response function,

$$g_m(\omega) = \frac{1}{(\omega - \omega_m) - i\alpha_m} \quad (3.2)$$

Here, ω_m is the modal resonance frequency and α_m is related to the modal loss factor by $2\alpha_m/\omega_m = \eta_m$.

If W is the mean square pure tone response, then

$$W(\omega) = \frac{1}{2} |y(\omega)|^2 \quad (3.3)$$

We shall assume that all modes are fairly lightly damped so that strong resonances occur at $\omega = \omega_m$. The expression for W may be written

$$W = \frac{1}{2} \sum_{m,n} b_m b_n g_m g_n^* \quad (3.4)$$

$$\approx \frac{1}{2} \sum_m b_m^2 |g_m|^2$$

where we have assumed that $g_m g_n^* \approx 0$, when $\omega_m \neq \omega_n$ for any ω . This is essentially the assumption of very small modal overlap. The expression for W is a superposition of "events" $|g_m|^2$ of magnitude $\frac{1}{2} b_m^2$ spaced along the frequency axis. For a flat panel, the average modal density is constant (Ref. 5), and if we assume a Poisson placement of modes along the axis, we can directly compute some needed statistical properties of W . We shall also assume that the damping is the same for all modes, $\alpha_m = \alpha = \text{const.}$

Rice has shown that the correlation function of a process like W has a correlation function given by (Ref. 6)

$$\phi_w(\xi) = \frac{1}{4} \overline{b^4} n_s(\omega) g^2 * g^2 \quad (3.5)$$

where "*" is the symbol for the convolution operation defined by

$$g^2 * g^2 = \int_{-\infty}^{\infty} d\omega |g(\omega)|^2 |g(\omega+\xi)|^2 \quad (3.6)$$

Since $|g|^2$ has a spectrum given by,

$$S_g(\tau) = e^{-\alpha|\tau|},$$

the spectrum of the convolution of $|g|^2$ is (Ref. 7)

$$G(\tau) = e^{-\alpha|\tau|} \cdot e^{-\alpha|\tau|} = e^{-2\alpha|\tau|}$$

The inverse of this spectrum is the convolution,

$$|g|^2 * |g|^2 = \frac{1}{\xi^2 + 4\alpha^2}$$

Placing this in Equation (3.5) and requiring that $\phi_w \rightarrow 1$ as $\xi \rightarrow 0$ gives

$$\phi_w(\xi) = \frac{4\alpha^2}{\xi^2 + 4\alpha^2} \quad (3.7)$$

The result Equation (3.7) is the same as that which Schroeder obtained for the case of high mode density given in Equation (2.5). This strongly suggests that the correlation function for μ is not dependent on modal spacing. Since the correlation function is given by Equation (3.7), the result of Equation (2.10) for the variance of band response is unchanged. The expression for m_w and σ_w will be altered however.

The mean value of W is (Ref. 8)

$$\begin{aligned} m_w &= \frac{1}{2} n_s(\omega) \overline{b^2} \int_{-\infty}^{\infty} d\omega |g(\omega)|^2 \\ &= \frac{\pi}{2\alpha} n_s(\omega) \overline{b^2} . \end{aligned} \quad (3.8)$$

The variance of W is given by (Ref. 9)

$$\begin{aligned} \sigma_w^2 &= \frac{1}{2} n_s(\omega) \overline{b^4} \int_{-\infty}^{\infty} d\omega |g(\omega)|^4 \\ &= \frac{\pi}{8\alpha^3} n_s(\omega) \overline{b^4} . \end{aligned} \quad (3.9)$$

The excitation coefficients b depend on the type of source used to drive the structure. If we use a shaker attached at a point \underline{x}^0 they are of the form

$$b \simeq B \sin m_1 \pi x_1 / l_1 \sin m_2 \pi x_2 / l_2 \sin m_1 \pi x_1^0 / l_1 \sin m_2 \pi x_2^0 / l_2 \quad (3.10)$$

We may form the moments of b by averaging over \underline{x} , \underline{x}^0 :

$$\begin{aligned} \overline{b^2} &= B^2 \left(\frac{1}{2} \right)^4 \\ \overline{b^4} &= B^4 \left(\frac{3}{8} \right)^4 = \left(\frac{3}{2} \right)^4 \overline{b^2}^2 \end{aligned}$$

Thus,

$$\begin{aligned} m_w &= m_v = \frac{\pi}{2\alpha} n_s \overline{b^2} \\ \sigma_w^2 &= \left(\frac{3}{2} \right)^4 \frac{m_v^2}{2\pi\alpha n_s} \end{aligned} \quad (3.11)$$

Using Equation (3.11) in Equation (2.10), we have finally,

$$\frac{\sigma_V}{m_V} = \left(\frac{3}{2}\right)^2 \left\{ \frac{f(N)}{n_s \Delta} \right\}^{1/2} \quad (3.12)$$

We note from Equation (3.12) that as the number of modes $n_s \Delta$ embraced by the exciting bandwidth is increased, the variation in response is diminished. This agrees with our intuition. Also, as the damping is diminished, N increases and $f(N)$ increases, rapidly for small N and more slowly as N rises above unity (see Figure 2.1). Thus, the variation in response increases as damping is reduced, again in agreement with our intuitive notions. The behavior in the low modal density region is therefore in sharp contrast with the behavior at high modal density as discussed in Section B.

The low density relative variation will equal the high density variation when

$$\sigma_w^2 = \left(\frac{3}{2}\right)^4 \frac{m_V^2}{2\pi a n_s} = 2m_V^2,$$

or,

$$2\pi a n_s = 81/32 = 2.5. \quad (3.13)$$

Since $2\pi a$ is the effective bandwidth of a mode, this represents an overlapping of 2 to 3 modes, which is consistent with Schroeder's criterion for the passage from non-overlapping to overlapping behavior, (Ref. 3). Of course, the non-overlap assumptions which have been made really preclude our full acceptance of any conclusions which apply the work of this section to a region of overlap above $n_s \cdot 2\pi a = 1$.

D. STATISTICAL ESTIMATION OF THE RESPONSE OF A HARMONIC OSCILLATOR ATTACHED TO A FLAT PLATE

The response of a simple oscillator attached to a structure of many degrees of freedom will be approached from the energy-statistical method developed by Lyon and Maidanik (Ref. 10). In subsection 1, we develop expressions for the power transfer between the oscillator and the structure. From these we compute the mean and the variance of the power flow, since as we indicate in subsection 2, this power flow governs the energy level of the oscillator when it is attached to the structure. Using the known mean and variance of the power flow in subsection 3, we assume

an appropriate distribution and compute confidence levels for the vibration levels. It is this last step which gives engineering value to the estimates since it defines a "safety factor" in terms of so many db which must be added to the mean value estimates in order to insure that the measured levels will fall below the estimate a certain fraction, say 95%, of the time.

1. Power flow between an oscillator and a flat plate

We assume that the single substructure mode - many structural mode interaction problem may be modelled by the simple system shown in Fig. 2.2. The transverse velocity u of the flat plate is governed by the equation

$$k^2 c_l^2 \nabla^4 u + \frac{\partial^2 u}{\partial t^2} + \beta_p \frac{\partial u}{\partial t} = \frac{1}{\rho_s} \frac{\partial p}{\partial t} \quad , \quad (4.1)$$

where k is the radius of gyration of the cross section, c_l is the longitudinal plate velocity, β_p is related to the loss factor η_p for the plate by $\beta_p = \eta_p \omega$, ρ_s is the surface density of the panel, and p is the force per unit area on the plate taken positive in the u direction. A homogeneous plate of thickness $h = 2\sqrt{3} k$ and area A_p has a modal density (in radian frequency space)

$$n = \sqrt{3} A_p / 2\pi c_l h \quad . \quad (4.2)$$

The pressure p will be divided into the random noise sources r which sustain the vibrations and the reaction force from the oscillator at the attachment point \underline{x}_0 . Thus,

$$\frac{\partial p}{\partial t} = \frac{\partial r}{\partial t} - \frac{df}{dt} \delta(\underline{x} - \underline{x}_0) \quad . \quad (4.3)$$

The eigenfunctions of the plate satisfy the following relations,

$$\left. \begin{aligned} \nabla^4 \psi_m &= k_m^4 \psi_m \\ \int_{A_p} \psi_m \psi_n d\underline{x} &= \delta_{mn} \end{aligned} \right\} \quad (4.4)$$

If we expand u , r and $\delta(\underline{x} - \underline{x}_0)$ in these functions,

$$\left. \begin{aligned} u &= \sum_m U_m(t) \psi_m(\underline{x}) \\ \delta(\underline{x} - \underline{x}_0) &= \sum_m \psi_m(\underline{x}_0) \psi_m(\underline{x}) \\ \frac{\partial r}{\partial t} &= \sum_m S_m(t) \psi_m(\underline{x}) \end{aligned} \right\} \quad (4.5)$$

then Equation (4.1) becomes

$$\frac{d^2 U_m}{dt^2} + \beta_p \frac{dU_m}{dt} + \omega_m^2 U_m + \rho_s^{-1} \psi_m^0 \frac{df}{dt} = S_m(t), \quad (4.6)$$

where, $\omega_m^2 = k_m^4 k_m^2 c_l^2$ and $\psi_m^0 = \psi_m(\underline{x}_0)$

The oscillator is shown in Figure 2.2 along with its mechanical diagram and mobility analog. If we consider the force on the mass to be the dependent variable, then its equation of motion is

$$\frac{d^2 f}{dt^2} + \beta_o \frac{df}{dt} + \omega_o^2 f - M\omega_o^2 \sum_m \psi_m^0 \frac{dU_m}{dt} = \omega_o^2 f_s(t). \quad (4.7)$$

Here, $\eta_o = \beta_o/\omega$ is the loss factor for the oscillator, and $\omega_o = (K/M)^{1/2}$ is the resonance frequency.

The symmetry between Equations (4.6) and (4.7) is improved by the following change in variables:

$$\left. \begin{aligned} \phi &= f(K/\rho_s)^{1/4} \\ \mu_m &= U_m(\rho_s/K)^{1/4} \\ \psi_m &= \psi_m(\rho_s K)^{-1/2} \end{aligned} \right\} \quad (4.8)$$

Using the new variables, the equations become

$$\frac{d^2 \mu_m}{dt^2} + \beta_p \frac{d\mu_m}{dt} + \omega_m^2 \mu_m + \psi_m^0 \frac{d\phi}{dt} = s_m(t) \quad (4.7a)$$

$$\frac{d^2 \phi}{dt^2} + \beta_o \frac{d\phi}{dt} + \omega_o^2 \phi - \sum_m \psi_m^0 \frac{d\mu_m}{dt} = \omega_o^2 \phi_s(t) \quad (4.8a)$$

Let us assume that the oscillator is excited by wideband noise, but the plate has no excitation other than by its attachment to the oscillator. The power received by the plate is:

$$P = \overline{fU_o} = \sum_m \psi_m^0 \overline{fU_m} = (\rho_s K)^{1/2} \sum_m \psi_m^0 \overline{\phi_{\mu_m}} \quad (4.9)$$

The cross moments $\overline{\phi_{\mu_m}}$ have been computed for the pair of Equations (4.7a) and (4.8a) in Reference 10. Their values are (Ref. 11)

$$\overline{\phi_{\mu_m}} = \frac{(\beta_o + \beta_p) \psi_m^0 \overline{(d\phi/dt)^2}}{(\omega_o^2 - \omega_m^2)^2 + (\beta_o + \beta_p)(\beta_o \omega_m^2 + \beta_p \omega_o^2)} \quad (4.10)$$

The summation (4.9) is subject to some uncertainties since one would not care to specify ψ_m^0 or ω_m^0 precisely for all possible experimental configurations. We therefore describe them statistically. The transferred power is

$$P = \frac{\bar{r}^2 (\beta_o + \beta_p)}{4\rho_s} \sum_m \bar{\psi_m^0}^2 \left[(\omega_o - \omega_m)^2 + (\beta_o + \beta_p)^2/4 \right]^{-1} \quad (4.11)$$

We assume that the frequencies ω_m are distributed along the frequency axis as a Poisson process with a mean value given by Equation (4.2). The mean value of P is (Ref. 8)

$$\begin{aligned} \bar{P} &= \frac{n \bar{\psi_m^0}^2 \bar{r}^2}{4\rho_s} (\beta_o + \beta_p) \int_{-\infty}^{\infty} \frac{d\omega}{(\omega - \omega_o)^2 + (\beta_o + \beta_p)^2/4} \\ &= \bar{r}^2 / R_{in} \end{aligned} \quad (4.12)$$

where

$$R_{in} = 4\rho_p c_p h^2 / \sqrt{3}$$

is the (real) input impedance of an infinite plate, (Ref. 12). Equation (4.12) may be considered the basis for mean value estimates of power flow from a shaker into a structure and the vibration of connected structures (Appendix III, Equation (2.3)).

In order to find the variation in estimated response, we will need the variance of P. It is (Ref. 9)

$$\sigma^2 = \frac{r^2 (\beta_o + \beta_p)^2 \overline{\psi_m^4} n}{16 \rho_s^2} \int_{-\infty}^{\infty} d\omega \left[(\omega - \omega_o)^2 + (\beta_o + \beta_p)^2 / 4 \right]^{-2}$$

(4.13)

$$= (\overline{\psi_m^4} / \overline{\psi_m^2})^2 m^2 / \pi (\beta_o + \beta_p) n.$$

The form of Equation (4.13) indicates fairly clearly the sources of variation and their effects. The first term is the effect of spatial variation; for two dimensional sinusoidal modes its value is 9/4. The second factor is that of irregularity in the number of modes which the oscillator is likely to encounter. The result is in the form of a central limit theorem which states that the standard deviation σ will diminish relative to the mean as the number of interacting modes

$$N = \pi n (\beta_o + \beta_p) \tag{4.14}$$

is increased.

2. Relation between power transfer and equilibrium vibration levels

To get the power balance equations for the system, one multiplies Equation (4.7a) by $-\dot{\mu}_m dt$ and Equation (4.8a) by $-\dot{\phi} dt$ and averages. The result is

$$\left. \begin{aligned} \beta_p \overline{\mu_m^2} + \overline{\psi_m^o \dot{\phi} \mu_m} &= \overline{\dot{s}_m \mu_m} \\ \beta_o \overline{\dot{\phi}^2} - \sum_m \overline{\psi_m^o \dot{\phi} \mu_m} &= -\omega_c^2 \overline{\dot{\phi}_s \int \dot{\phi} dt} \end{aligned} \right\} \tag{4.15}$$

In Reference 10, it was shown that if $\phi_s = 0$ and s_m is a set of wide band random noise sources, then the power flow into the oscillator is

$$P = \sum_m \psi_m^0 \overline{\phi \mu_m} = \sum_m (\theta_m - \theta_o) \beta_m^{\text{coup}}$$

where $\theta_m = \overline{\mu_m^2}$ and $\theta_o = \overline{\phi^2}$. If we can assume that the sources s_m will keep all the structure modes at the same energy level $\theta_m = \theta_p = \text{const}$, then

$$\beta_o \theta_o = (\theta_p - \theta_o) \beta_{\text{coup}}$$

where

$$\beta_{\text{coup}} = \sum_m \beta_m^{\text{coup}}$$

or

$$\theta_o = \theta_p \frac{\beta_{\text{coup}}}{\beta_{\text{coup}} + \beta_o} \quad (4.16)$$

where β_{coup} is essentially the sum which was evaluated as P in subsection 1. We note that if $\beta_{\text{coup}} \ll \beta_o$, the statistics of β_{coup} are those of θ_o . In the event that $\beta_{\text{coup}} \gg \beta_o$, one would have $\theta_o = \theta_p$ and no variation would exist.

Our estimates of variance and mean values in the previous subsection therefore require equal energy in the plate modes if we expect then to predict the substructure (oscillator) response. If the s_m 's are caused by a point source at position \underline{x} , then the variance in response will contain an additional factor of variation $\frac{\psi_m^4}{\psi_m^2}$.

3. Confidence levels for estimates of random response

We have developed expressions for the mean and variance of power flow or response when an oscillator is attached to a flat plate. We should now like to use these in such a way that confidence levels for the estimated response may be computed. In particular, if we calculate an average response, then we might ask, "by how many db should one increase this estimate so that the estimate is not exceeded in, say, 95% of the cases?" Our purpose in this subsection is to answer this question.

We do not know the probability density $\phi(P)$, but if we did, the above requirement would be met by setting our estimate at A, such that

$$\int_0^A \phi(P) dP = 0.95 = CL \quad (4.17)$$

We shall get around our ignorance of ϕ by assuming a form for it. We require a density function which is defined for positive arguments only, and has parameters easily related to the mean and variance. These requirements are met by the gamma distribution,

$$\phi(x) = \frac{x^{\alpha-1} e^{-x/\lambda}}{\lambda^\alpha \Gamma(\alpha)} \quad (4.18)$$

where (Ref. 13)

$$m = \lambda\alpha, \quad \sigma^2 = \lambda^2\alpha$$

One has then

$$\alpha = \frac{m^2}{\sigma^2}, \quad \lambda = \frac{\sigma^2}{m} \quad (4.19)$$

Changing variables to $y = x/\lambda$, the condition Equation (4.17) becomes

$$\Gamma^{-1}(\alpha) \int_0^{A/\lambda = B} dy y^{\alpha-1} e^{-y} = \frac{\gamma(\alpha, B)}{\Gamma(\alpha)} = CL \quad (4.20)$$

where $\gamma(\alpha, B)$ is the incomplete gamma function, (Ref. 14).

The function Equation (4.20) is plotted by Jahnke and Emde (Ref. 15) for various values of CL. Using their values, we have plotted curves of constant CL in Figure 2.4, with the ratio of squared mean to variance as the abscissa, and $10 \log A/m$ as the ordinate, where

$$A/m = B/\alpha . \quad (4.21)$$

The curves in Figure 2.4 essentially tell us how many db to add to the mean value estimate in order to ensure that a fraction CL of the measured values of response will fall below the estimate. Thus for example, if

$$N = \pi n (\beta_o + \beta_p) = 10 ,$$

then $\alpha = 4.44$ and one would have to add 2.8 db for a confidence level of 95% or 3.8 db for a confidence level of 99%. If the plate is driven by a point source shaker so that an additional variance factor arises from the modal energy uncertainty, then the relevant value of α is

$$\alpha = \left(\frac{4}{9}\right)^2 N = 1.96 .$$

Referring to Figure 2.4, a confidence level of 95% would require that we add 3.9 db to the mean value estimate. For 99% confidence, we would have to add 5.2 db.

NOTES AND REFERENCES FOR APPENDIX II

1. D. U. Noiseux, J. J. Coles, N. Doelling, R. H. Lyon, "Response of electronics to intense sound fields," Report No. 871, Bolt Beranek and Newman Inc., Cambridge, Massachusetts, July, 1961, Section III.
2. Reference 1, Section IV.
3. M. R. Schroeder, "On frequency response curves in rooms," J. Acoust. Soc. Am. 34, 1, 76-80, January, 1962. Note that our Equation (2.5) is the transform of Schroeder's Equation (11).
4. M. R. Schroeder, "The statistical parameters of the frequency response curves of large rooms," Acustica 4, Beiheft 2, 594, 1954. In German with English summary.
5. G. Maidanik, "Response of ribbed panels to reverberant acoustic fields," J. Acoust. Soc. Am. 34, 6, 809, June, 1962, Equation (1.4).
6. S. O. Rice, "Mathematical analysis of random noise," Contribution to Noise and Stochastic Processes, Ed., N. Wax, (Dover Publications, Inc., New York, 1954) Equation (2.6-2).
7. Reference 6, Equation (2.6-4).
8. Reference 6, Equation (1.3-4).
9. Reference 6, p. 150.
10. R. H. Lyon and G. Maidanik, "Power flow between linearly coupled oscillators," J. Acoust. Soc. Am. 34, 5, 623, May. 1962.
11. See Reference 10. The arguments for reducing the one oscillator-many mode interaction problem to separate interactions of the modes are given in Section IX. The covariance $\overline{\mu_m \phi}$ used here is found from setting $A = C = 0$ in Equation (2.10).
12. See Appendix I.

13. A. M. Mood, Introduction to the Theory of Statistics, (McGraw-Hill Book Co., Inc., New York, 1950) Sec. 6.3.
14. A. Erdelyi, et al, Higher Transcendental Functions, Vol. II, (McGraw-Hill Book Co., Inc., New York, 1953) Sec. 9.1, Equation (1).
15. Jahnke, E., and Emde, F., Tables of Functions with Formulae and Curves, (Dover Publications, New York, 1945).

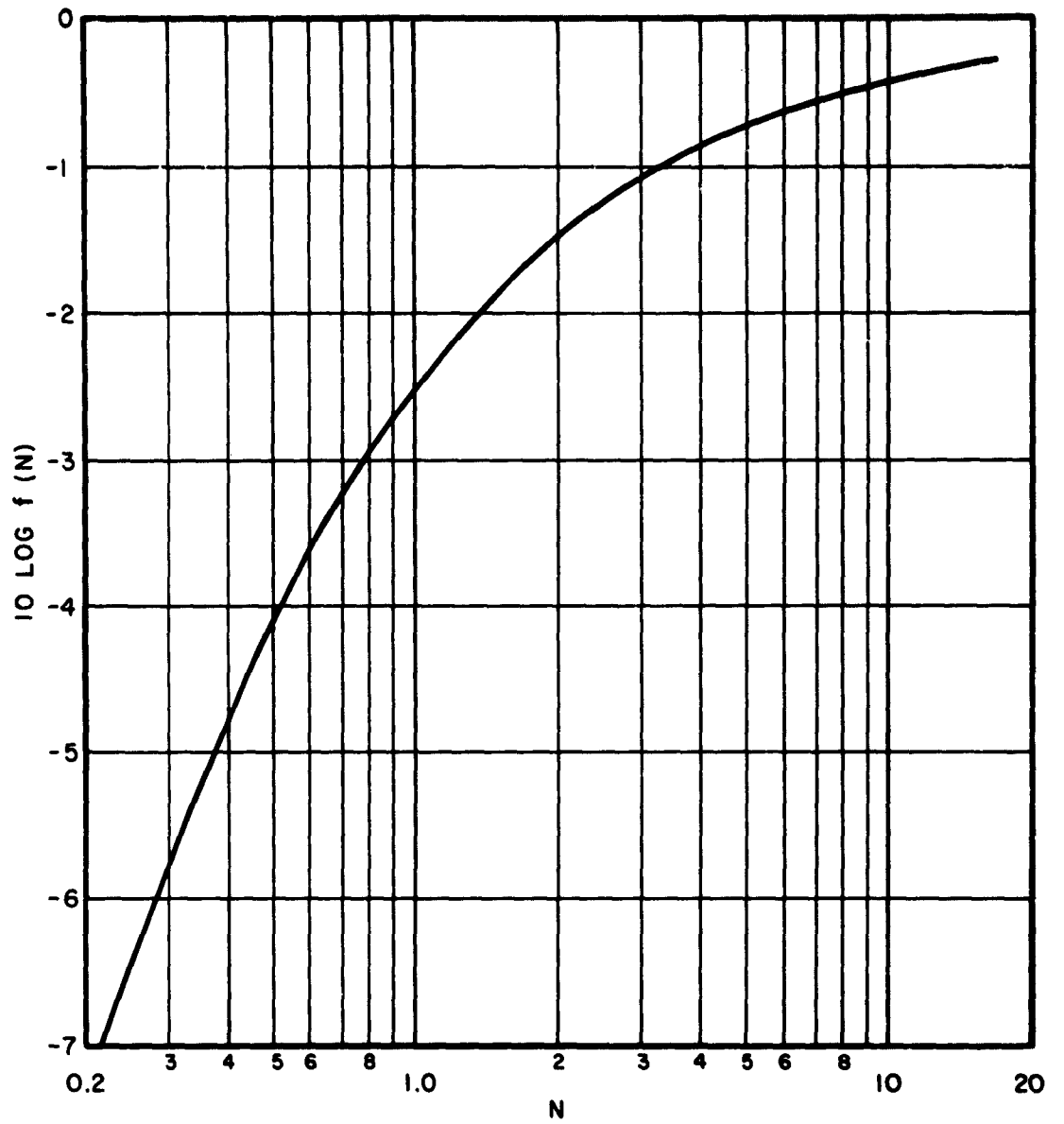


FIG. 2.1 GRAPH OF $10 \text{ LOG } f(N)$

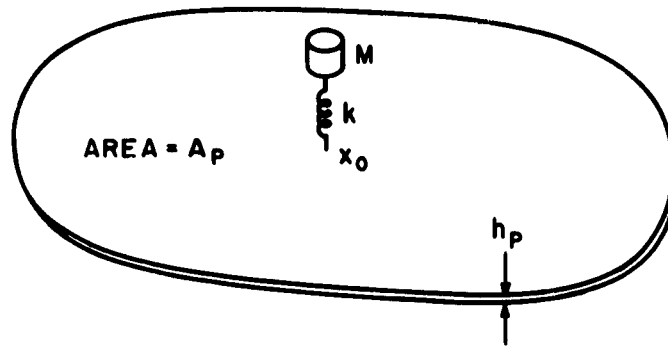


FIG. 2.2 DIAGRAM OF PLATE WITH ATTACHED OSCILLATOR

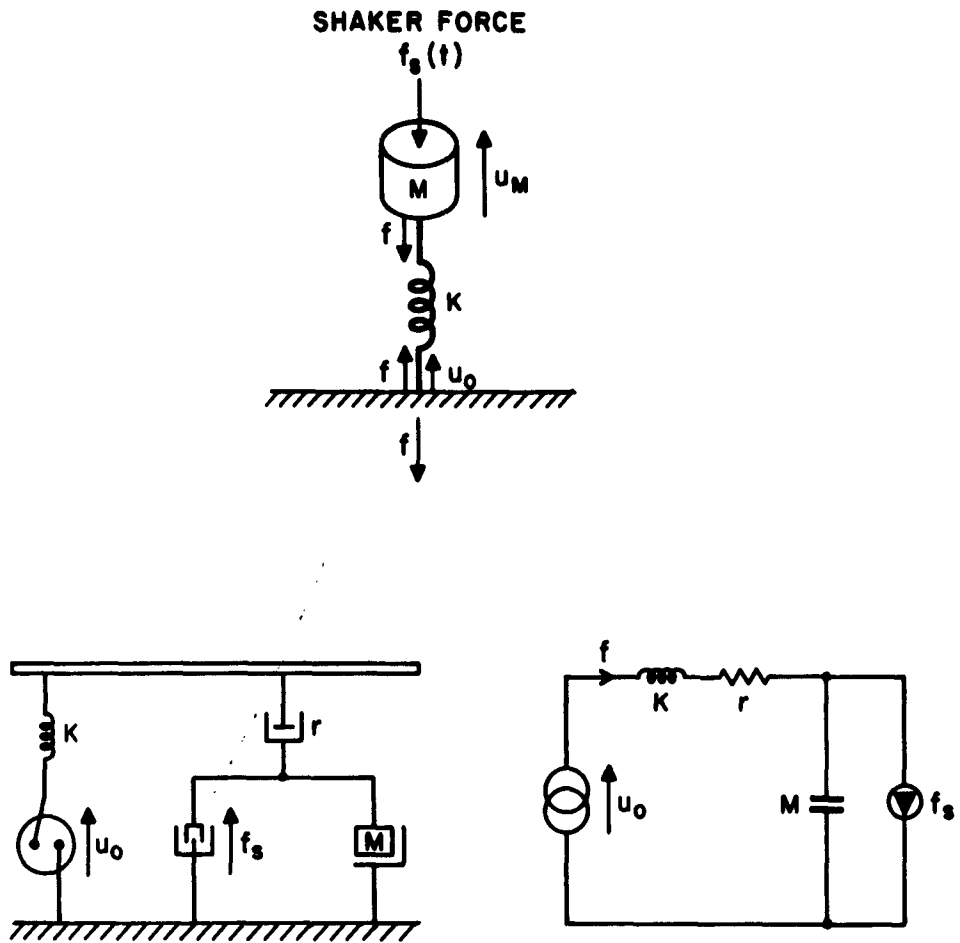


FIG. 2.3 OSCILLATOR SKETCH, MECHANICAL DIAGRAM, AND MOBILITY ANALOG EQUIVALENT CIRCUIT

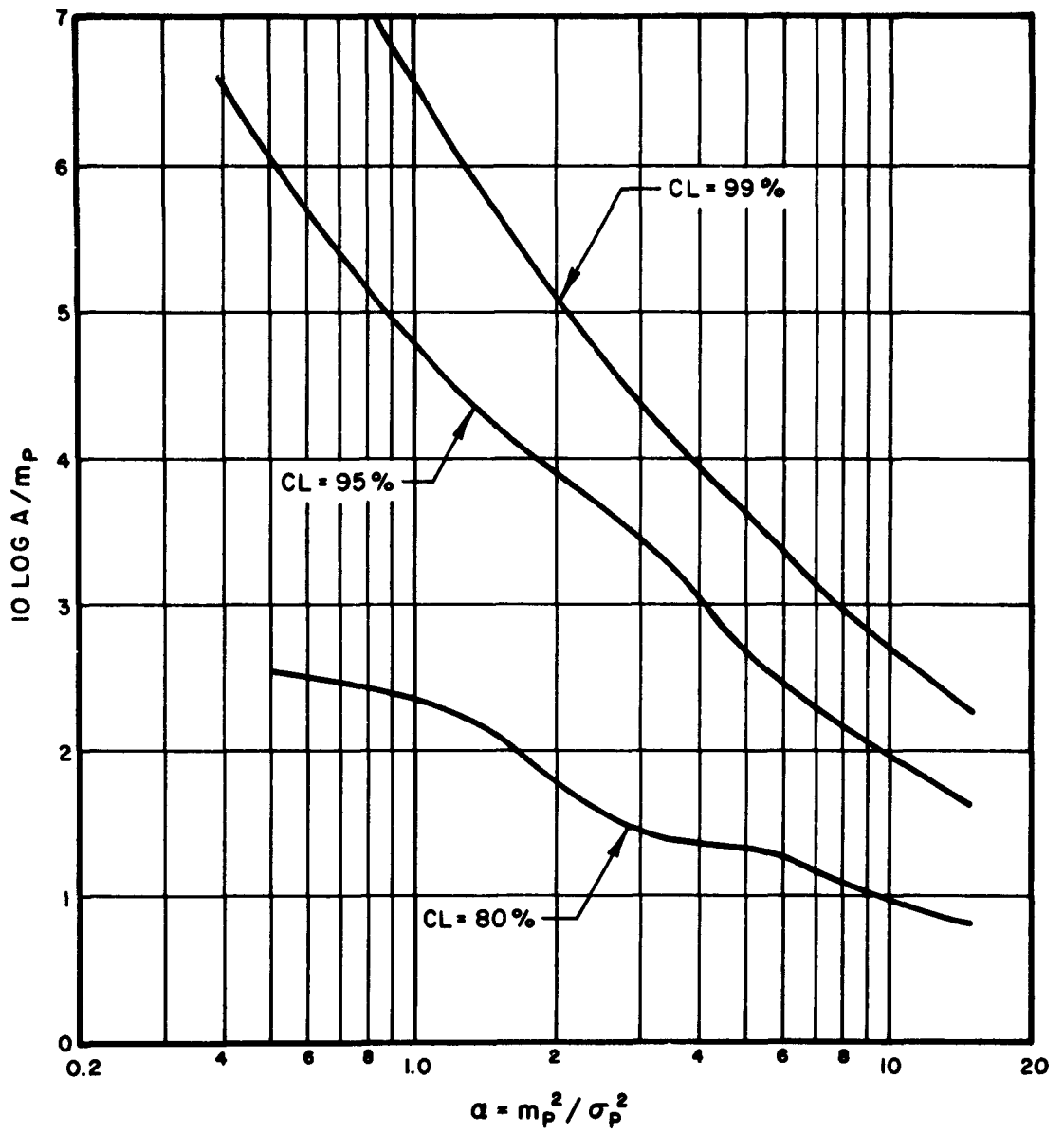


FIG. 2.4 SAFETY FACTOR IN ESTIMATION REQUIRED TO ACHIEVE GIVEN CONFIDENCE LEVEL

APPENDIX III

ENERGY SHARING BETWEEN CONNECTED STRUCTURES

A. INTRODUCTION

When large, complex structures are designed to operate in environments that may cause them to vibrate (e.g., intense sound fields, boundary layer turbulence, etc.), the design engineer is usually concerned with the response of a particular substructure that may be susceptible to malfunction (e.g., components of the structures that carry electronic equipment). We wish to develop methods for estimating the vibration of substructures attached to large complex structures. We define a large complex structure such that it has high modal density and its modes are fairly uniformly distributed in frequency space. We assume that the substructure has its own modal density and that the method of attachment of the substructure to the large structure is known. We further assume that the vibration of the structure is predominantly resonant, i.e., the modes of vibration of both the structure and substructure are not critically damped. Under this assumption one may treat the interaction between the structures by considering the interaction of one set of oscillators (modes) that is coupled in a known manner to another set.

The power flow between two linearly coupled oscillators has been studied by Lyon and Maidanik (Ref. 1). The formalism has been extended to cover the case of the power flow between two sets of coupled oscillators. The theory has also been applied specifically to the interaction between a reverberant acoustical field (considered to have a very high modal density), and a structure, e.g., a beam, a panel or a combination of both, (Ref. 2). It is possible to treat the connected structure problem by the same methods, as we shall show.

The coupling is strongest between modes of the structure (high modal density assumed) and a mode of the substructure when they lie close in frequency space. Modes which lie outside each others passbands are usually weakly coupled. In a given frequency band centered about a given ω (ω = angular frequency), if θ_{ss} is the modal energy of the substructure and θ_s is the modal energy of the structure, then if the structure is excited by external source fields, the relation between θ_{ss} and θ_s can be shown to be (Ref. 1)

$$\theta_{ss} = \theta_s \mu_s^{ss} \quad (1.1)$$

where

$$\mu_s^{ss} = \frac{\eta_c}{\eta_c + \eta_{ss}} \quad (1.2)$$

The ratio (1.2) is called the coupling factor for the substructure; η_c and η_{ss} are the loss factors associated with the coupling and the substructure damping respectively. While η_{ss} is related to the power dissipated internally, η_c is related to the power lost (or gained) by the substructure to (or from) the structure via the coupling (c.f., $R_{rad} = \omega M_p \eta_{rad}$ for the acoustic case (Ref. 1)).

Equation (1.1) states that in the steady state condition the modes of the substructure attain modal energies that are a fraction μ of the modal energy of the structure. For $\eta_c \gg \eta_{ss}$, $\theta_{ss} \sim \theta_s$ and for $\eta_c \ll \eta_{ss}$, $\theta_{ss} \ll \theta_s$.

Equation (1.1) is an approximate statistical formula, (Ref. 1). The approximation is better as the number of interacting modes in a given frequency band increases. This is so because the formula is derived by averaging a summation over modes that lie in the frequency band (e.g., octave or third-octave). Thus one would expect the approximation to be better the higher the modal density of the structures and the wider the frequency band chosen. One could get an idea of the errors involved in the smoothing procedures by computing the variances of the fluctuations in the responses of the structure and substructures; this is being reported in Appendix II. In this Appendix for the present we concentrate on examining whether the general assumptions and ideas expressed with respect to Equation (1.1) are in keeping with experimental data.

B. BEAM CANTILEVERED TO FLAT PLATE

To test Equation (1.1), we choose to examine a beam cantilevered to a flat plate. The beam and the plate are so chosen that the coupling loss factor η_c may be conveniently estimated. Moreover, the dimensions of the beam and the plate are such that the conditions for the validity of Equation (1.1) are approximately satisfied. Below we discuss briefly the theoretical and experimental results involved in the test.

1. Theoretical Considerations

To determine η_c , we assume that the beam is excited by an external source, and we calculate the power loss to the plate via the coupling. The power flow into the plate from the beam is given by

$$P_{bp} = \overline{M^2} \operatorname{Re} \left(\frac{1}{Z_p^M} \right) , \quad (2.1)$$

where Z_p^M is the moment impedance of the plate as seen by the beam at the junction and $\overline{M^2}$ is the mean square moment generated at the junction by the vibration of the beam.

In terms of η_c , the power that the beam loses to the plate through the coupling is given by

$$P_{bp} = \eta_c \omega M_b \overline{v_b^2} , \quad (2.2)$$

where $\overline{v_b^2}$ is the mean square velocity of the beam averaged in time and space and M_b is the total mass of the beam.

Equating Equations (2.1) and (2.2) we have

$$\eta_c = \frac{\overline{M^2}}{\omega M_b \overline{v_b^2}} \operatorname{Re} \left(\frac{1}{Z_p^M} \right) . \quad (2.3)$$

If a typical dimension of the junction is small compared to a wavelength in the beam and plate, then (Ref. 2)

$$\operatorname{Re} \left(\frac{1}{Z_p^M} \right) = \frac{3\omega}{4\rho_p h_p^3 c_p^2} , \quad (2.4)$$

where ρ_p is the density, h_p is the thickness, and c_p is the longitudinal velocity of the plate.

We have now to determine $\overline{M^2}$. Consider the analog circuit of Figure 3.1 depicting the coupling between the plate and beam. The flow quantity is the angular velocity and the potential drop is the moment M . Z_p^M and Z_b^M are the moment impedances of the plate and the beam as seen by the beam and plate respectively. We note from Figure 3.1 that the mean square moment is given by

$$\overline{M^2} = \overline{M^{2b}} \left| \frac{z_p^M}{z_b^M + z_p^M} \right|^2 \quad (2.5)$$

where $\overline{M^{2b}}$ is the mean square moment of the beam, $\overline{M^{2b}}$ is related to the mean square velocity on the beam, v_b^2 by the equation

$$\overline{M^{2b}} = 4\rho_b^2 c_b^2 \kappa_b^2 S_b^2 v_b^2 \omega^{-2} \quad (2.6)$$

where ρ_b is the density, c_b the longitudinal velocity, κ_b the radius of gyration and S_b the cross-sectional area of the beam.

Combining Equations (2.3), (2.4), (2.5), and (2.6) we obtain

$$\eta_c = \frac{h_b^3 w}{4h_p^3 l} \xi \quad (2.7)$$

where h_b is the thickness, w the width, l the length of the beam, and

$$\xi = \left| \frac{z_p^M}{z_b^M + z_p^M} \right|^2 .$$

The expression for ξ may be written in the form (Ref. 2)

$$\xi = \frac{1}{1 + \Lambda(1+i)(1-i\Gamma)} ,$$

where

$$\Lambda = \frac{\rho_b h_b^3 c_b^2 (wk_b)}{32\rho_p h_p^3 c_p^2} ,$$

k_b being the wavenumber for the beam. For a circular beam of radius r , $\Gamma = \frac{4}{\pi} \log_e (k_p r) [k_p r \ll 1]$, (Ref. 2). For a rectangular beam the expression for Γ is lacking. We assume that for our arrangement (see Figure 3.2) the absolute value of Γ is the order of unity. Thus, for the case under consideration here ($\rho_p = \rho_b$, $h_p = h_b$, $c_p = c_b$, $w = 4$ cm and $k_b \approx 0.7$ cm⁻¹ at 4 kc), we may set $\xi = 1$ in the frequency range from 50 cps to 12 kc. One should note that a better approximation may lead to somewhat lower values of ξ and hence smaller η_c .

2. Experimental Considerations and Results

Equation (1.1) as it is given is not convenient for practical purposes since one cannot measure θ_{ss} and θ_s directly. We have to express the modal energies in terms of measurable quantities. The energy of a structure (a beam or a plate) in a given frequency band (e.g., third-octave or octave) is given by

$$E_s = \frac{M_s S^a}{\omega^2} \Delta\omega \quad , \quad (2.8)$$

where S^a is the acceleration spectral density of the structure in the frequency band $\Delta\omega$, ω is the center frequency of the band and M_s is the total mass of the structure. The modal energy of the vibration of the structure is given by

$$\theta_s = \frac{E_s}{n(\omega)\Delta\omega} = \frac{MS^a}{\omega^2 n(\omega)} \quad (2.9)$$

where $n(\omega)$ is the average modal density in the band $\Delta\omega$.

Substituting Equation (2.9) in Equation (1.1) and making the appropriate identification of the quantities, we obtain

$$\frac{S_b^a}{S_p^a} = \frac{n_b(\omega)M_p}{n_p(\omega)M_b} \frac{\eta_c}{\eta_c + \eta_b} \quad , \quad (2.10)$$

where subscripts p and b refer to quantities related to the plate and the beam respectively.

Equation (2.10) is now in a form where the parameters involved are measurable.

The beam-plate system is shown in schematic form in Figure 3.2. The dimensions of the aluminum beam are 95" x 1.5" x 1/8" and those of the plate 72" x 48" x 1/8". The choice of a rather thick beam and plate is made to avoid excessive loading of the structures by the accelerometers at high frequencies. The beam is attached perpendicularly to the plate by epoxy. The positions on the plate and beam where measurements were taken is indicated in Figure 3.2 by the circled numbers.

The modal density of the plate, n_p , is measured by exciting the plate with a shaker and counting pure tone resonances. It is found that the modal density of the plate conforms closely to its asymptotic theoretical value, which is given by (Ref. 3)

$$n_p(\omega) = \frac{\sqrt{3} A_p}{2\pi c_p h_p}, \quad (2.11)$$

where A_p is the area of the plate.

For our plate $n_p(\omega) \sim 3.8 \times 10^{-2}$ modes/radian per second. Deviation from the value of $n_p(\omega)$ as given by Equation (2.11) occurs only below about 50 cps. We shall not be concerned with frequencies below 50 cps.

The modal density of the beam is measured in the same way. It is found that the measured modal density of the beam agrees fairly well with the asymptotic theoretical value given by the formula (Ref. 3)

$$n_b(\omega) = \frac{l}{\pi} \left(\frac{\sqrt{3}}{\omega c_b h_b} \right)^{1/2} \quad (2.12)$$

It is of interest to note that above 6 kc the modal density of the beam exceeds the value which is given by Equation (2.12) and slowly approaches the modal density of a plate as the frequency is increased. From these measurements the quantity

$$10 \log_{10} \frac{n_b(\omega) M_p}{n_p(\omega) M_b} \quad (2.13)$$

is determined. This quantity is given in graphical form in Figure 3.4. The factor given by Equation (2.13) represents the ratio between the acceleration spectral densities of the plate and the beam (in db) for the case of "thermal equilibrium" i.e., equipartition of modal energy ($\theta_{ss} = \theta_s$).

The quantity η_b is determined by measuring the reverberation time of the beam (unattached)(Ref. 4). It is related to the reverberation time T_b by the equation

$$\eta_b = \frac{13.8}{\omega T_b} . \quad (2.14)$$

The loss factor η_b is determined for two cases, an undamped beam and a damped beam. The damping was achieved by attaching damping tape to the beam. Using the theoretical values of η_c [Equation (2.7) with $\xi = 1$] and the experimental values of Equations (2.13) and (2.14), S_b^a/S_p^a is determined from Equation (2.10). The results are given in graphical form in Figures 3.3 and 3.4.

We then proceed to measure the quantity S_b^a/S_p^a directly in order to compare it with the values obtained above. This constitutes a test of the validity of Equation (2.10).

A block diagram of the system for measuring S_b^a/S_p^a is shown in Figure 3.5. The acceleration is measured (in third-octave and octave bands) successively at selected points on the plate and beam (see Figure 3.2) and simultaneously at point P on the plate. The difference (in db) between the acceleration at a given point and at point P is thus obtained. In a given frequency band these differences are averaged over all the selected points of the beam and, separately, over all the selected points on the plate. The difference between these averages gives the value of S_b^a/S_p^a in the frequency band. The values of S_b^a/S_p^a so obtained are given in graphical form in Figures 3.3 and 3.4 for two cases of damping; the two cases are the same as those for which reverberation time measurements were made.

It should be pointed out that the beam and the plate are found to be fairly reverberant in the sense that the accelerations (normalized by the acceleration at point P) taken at the selected points on the plate and the beam are found to be within 1 or 2 db of their averaged values. Note that this indicates that the vibration of the structures is predominantly resonant, a necessary condition for the validity of Equation (2.10).

The comparison between the direct measurement of S_b^a/S_p^a and the indirect measurement (where the right-hand side of Equation (2.10) is computed) is shown graphically in Figures 3.3. and 3.4. We feel the agreement between the values would be satisfactory as an engineering estimate. The point-to-point variations are in some cases, however, quite large. It was pointed out earlier that when the number of modes either in the plate and/or the beam

that participate in the coupling in any given frequency band is not large, fluctuations from the ideal case, which Equation (2.10) represents, are to be expected. Although the number of modes in the plate in any given third-octave band is fairly large, the number of beam modes is rather small. It is interesting to note that the fluctuations are greatly suppressed when measurements are conducted in octave instead of third-octave bands.

The results obtained indicate that the method developed above for estimating the vibrations of substructures may prove fruitful. Some refinements, especially with respect to estimating variances from the average values, would prove useful.

C. THE VIBRATION OF CONNECTED PANELS

1. Introduction

We shall now consider a connected structure which is a typical part of electronic packages. The racks, housings, and chassis of electronics systems, for example, are made up of plates or panels. We ask how much a subpanel will vibrate when its mounting rack is randomly excited. In order to answer this question eventually, we investigate here the flow of vibrational power between plates which are attached to each other by welded seams. We do not intend to explore each of the great number of joints between plates which are in use but rather to apply the general methods which have been previously outlined to a few types of connection.

Our fundamental formula is the energy ratio of two coupled modes, given in Equation (1.1). If the structures are reverberant, as we shall assume, we can eliminate the modal energies in favor of the "energy velocity" spectral densities and obtain

$$\frac{S_{ss}^v}{S_s^v} = \frac{n_{ss}}{M_{ss}} \cdot \frac{M_s}{n_s} \mu_s \quad (3.1)$$

where n is the modal density and M the mass of the respective structure.

For a flat plate, the modal density is

$$n = \frac{\sqrt{3} A}{2\pi h c_p} \quad (3.2)$$

where A is the (one-side) surface area, h the thickness of the plate, and c_l is the plate longitudinal wave velocity. The mass of the plate is $M = \rho Ah$, where ρ is the mass density. Hence, one obtains for connected plates

$$\frac{S_{ss}^v}{S_s^v} = \frac{\left(\rho h^2 c_l\right)_s}{\left(\rho h^2 c_l\right)_{ss}} \mu_s^{ss} \quad (3.3)$$

For plates of the same material we have simply

$$\frac{S_{ss}^v}{S_s^v} = \left(\frac{h_s}{h_{ss}}\right)^2 \mu_s^{ss} \quad (3.4)$$

This formula allows us to calculate the vibration level of the substructure if we know the thickness ratio and the coefficient μ_s^{ss} .

The determination of μ_s^{ss} will occupy us in the next two sections. If the substructure is excited, then μ_s^{ss} may be defined in terms of the power it loses by transmission and dissipation in the following manner

$$\mu_s^{ss} = \frac{\text{Power transferred to structure}}{\text{Total power lost}} \quad (3.5)$$

If these quantities are interpreted in terms of loss factors, Equation (1.1) results. Besides other results, we will present in subsection 2. theoretical expressions for the coupling loss factor of a plate which is clamped to a second plate. In subsection 3. we will report related measurements. The technique used in subsection 2. is wave theory. The plates are taken as infinitely large and a reverberant field is simulated by averaging over all directions. The boundary absorption equations used in subsection 3. are derived from a plate analogy to room acoustics. The absorption is obtained by measuring the reverberation time.

2. Flexural Wave Transmission between Clamped Panels

We consider a thin infinite half-plate 1 joined under a right angle to a thin infinite plate 2 (Figure 3.6). We assume that the plates are joined as if they were made from one piece. The joint may be approximated by a continuous welded or soldered seam.

Let u, v, w , be the displacements in the directions x, y, z . For small displacements $v \equiv 0$. At the joint $x = 0, z = 0$, the transverse displacements of both plates must vanish, $u = 0, w = 0$, (u refers to plate 2 and w to plate 1, but it is not necessary to use indices). The conservation of the right angle demands that $\partial w / \partial x = -\partial u / \partial z$. Let G be the moment (per unit length) acting on plate 1 at the joint (Figure 3.7).

From Love (Ref. 5) the bending moment along the straight edge of a plate is

$$G = -D[\partial^2 w / \partial n^2 + \sigma \partial^2 w / \partial s^2] \quad (3.6)$$

where n is the coordinate out of the edge ($\equiv x$) and s the coordinate along the edge ($\equiv y$), and

$$D = \rho c_p^2 h^3 / 12 \quad (3.7)$$

is the flexural stiffness of the plate. Applying this to each of the three half plates we obtain

$$D_1 \partial^2 w / \partial x^2 = D_2 (\partial^2 u / \partial z^2)_{-0} - D_2 (\partial^2 u / \partial z^2)_{+0} \quad (3.8)$$

Our set of boundary conditions is now complete.

The differential equation for small transverse vibrations of a thin plate is $[D \nabla^4 + \rho h \partial^2 / \partial t^2] w = 0$. For harmonic time dependence $\exp i\omega t$ and $\exp(-ik_y s \sin \alpha)$ on y we get the solutions $\exp(\pm ik_x \cos \alpha)$ and $\exp(\pm k_x \sqrt{1 + \sin^2 \alpha})$ in x . We calculate the transmission of a single wave

$$w = \exp(i\omega t - ik_1 y \sin \alpha - ik_1 x \cos \alpha), \quad (3.9)$$

incident in plate 1 at an angle of incidence α (Figure 3.6). Satisfying the boundary conditions we find for the wave transmitted into plate 2,

$$u = C \exp(i\omega t - ik_2 y \sin\beta - ik_2 z \cos\beta) \quad (3.10)$$

where

$$C = -(1+A) k_1 r / k_2 \quad (3.11)$$

$$= -2i(k_1 r / k_2) \cos\alpha [i \cos\alpha - \sqrt{1 + \sin^2\alpha} + r(i \cos\beta - \sqrt{1 + \sin^2\beta})]^{-1}$$

$$r = D_1 k_1 / 2D_2 k_2, \quad (3.12)$$

and A is the amplitude of the reflected wave. To preserve the dependence on y the angles α and β are related by

$$k_1 \sin\alpha = k_2 \sin\beta \quad (3.13)$$

The mean square velocity on plate 2 is

$$\begin{aligned} v_2^2 &= \frac{1}{2} \omega^2 |C|^2 \\ &= \frac{(\omega k_1 r / k_2)^2 \cos^2\alpha}{1 + r \sqrt{1 - \sin^2\alpha} \sqrt{1 - (k_1/k_2)^2 \sin^2\alpha} + r \sqrt{1 + \sin^2\alpha} \sqrt{1 + (k_1/k_2)^2 \sin^2\alpha} + r^2} \end{aligned} \quad (3.14)$$

If the transmission from plate 1 into plate 2 is small, we can take the amplitude of the reflected wave as $A = -1$, so that the squared velocity, averaged over plate 1, is

$$v_1^2 = \omega^2 \quad (3.15)$$

which is independent of α .

In a reverberant and diffuse field waves come from all directions with equal probability. The angular average of Equation (3.14) can be readily found in two special cases. For equal plates

$$\frac{\langle v_2^2 \rangle_\alpha}{v_1^2} = \frac{1}{9} \quad (3.16)$$

and for plate 1 much thinner than plate 2 ($k_1 \gg k_2$, $D_1 \ll D_2$, $r \ll 1$).

$$\frac{\langle v_2^2 \rangle_\alpha}{v_1^2} \doteq \frac{1}{2\pi} \left(\frac{r k_1}{k_2} \right)^2 \left[2 \arcsin \frac{k_2}{k_1} + \sin 2 \arcsin \frac{k_2}{k_1} \right] \doteq \frac{k_1^3 D_1^2}{2\pi k_2^3 D_2^2} \quad (3.17)$$

The average power per unit boundary length carried by a wave incident at the angle α (with amplitude 1) equals the average energy density

$$E = 2\rho h\omega^2 \quad (3.18)$$

times the group velocity

$$c_g = [\partial k / \partial \omega]^{-1} = 2\omega/k \quad (3.19)$$

times $\cos \alpha$. The corresponding power transmitted to plate 2 (and hence lost to plate 1) is

$$P_{\text{lost}} = |C|^2 \rho_2 h_2 \omega^3 k_2^{-1} \cos \beta \quad (3.20)$$

The ratio of the angular averages is the absorption coefficient

$$\gamma = \frac{r}{2} \int_{-\pi/2}^{\pi/2} \frac{\cos^2 \alpha \sqrt{1 - (k_1/k_2)^2 \sin^2 \alpha} \, d\alpha}{1 + r \sqrt{1 - \sin^2 \alpha} \sqrt{1 - (k_1/k_2)^2 \sin^2 \alpha} + r \sqrt{1 + \sin^2 \alpha} \sqrt{1 + (k_1/k_2)^2 \sin^2 \alpha} + r^2} \quad (3.21)$$

which can be calculated readily in two special cases. (The integrand is to be taken as zero where it is complex.) For equal plates we find

$$\gamma = 4/27 \quad , \quad (3.22)$$

and for plate 1 much weaker than plate 2

$$\gamma \doteq \frac{r}{4} \left[2 \arcsin \frac{k_2}{k_1} + \sin 2 \arcsin \frac{k_2}{k_1} \right] \doteq \frac{D_1}{2D_2} \quad (3.23)$$

(We are looking at plate 2 as a boundary absorber attached to plate 1. Note that this step is an intermediate step in the calculation of μ_3^{SS} which in turn is needed to calculate the excitation of plate 1 when plate 2 is driven.)

It remains to relate γ to η_c . This is easily done using the formula, (Ref. 6) for the reverberation time T

$$\frac{2.2}{T} = \frac{\eta \omega}{2\pi} + \frac{\gamma c L}{2\pi A} \quad , \quad (3.24)$$

where L is the length of the absorbing boundary. We may interpret the transmission as a coupling loss factor

$$\eta_{c1} = \frac{\gamma c_{g1} L}{\omega A_1} \quad (3.25)$$

which, together with the internal loss factor η_1 allows us to compute the coupling factor

$$\mu_2^1 = \frac{\eta_{c1}}{\eta_{c1} + \eta_1} \quad , \quad (3.26)$$

with plate 1 assuming the role of the substructure and plate 2 the role of the structure.

3. Experimental Study

Measurements were made on one aluminum plate and on two steel plates ("half plates") joined to heavier plates of similar material. The light plates were cut irregularly to promote diffuse conditions. The heavier plates were damped to approximate infinite plates when seen from the attached light plate.

The light plate was struck and the resulting vibration was sensed with an accelerometer (Glennite 314). After filtering through a third-octave band filter set (B+K 1609) the decay time was measured (Ref. 4) (BBN Reverberation Time Meter). The recorded times were converted into loss factors and absorption coefficients according to Equations (3.25) and (3.26). The results are plotted in Figures 3.8-10 together with theoretical values of γ from Equation (3.26).

We started with a thin aluminum plate which we glued to a heavy one by means of an artificial resin (Fig. 3.8). The measured values of the absorption coefficient turned out to be large in comparison with theory. We suspected that some imperfections in the joint or the glue itself was causing the excess absorption. This suspicion was confirmed when we measured the total loss factor η' of the same plate glued to a heavy steel bar. The difference between η' and the free plate loss factor η_1 represents the losses of the joint and is considerable.

We consequently went from the glued joint to an all-metal joint. Because of the large size of the plates we had difficulties in the production of the test object. The next plate we tested was a thin steel plate welded to a heavy one (Figure 3.9).

The welded joint was not uniform and we found again absorption values which were higher than the predicted ones. We finally obtained a very good weld on a steel plate joined to another one about three times as thick. In this case the agreement between experiment and theory was excellent. It seems that the slightly increased torsional stiffness of the joint (due to the welded depositions) did not make the theory unapplicable.

Good agreement between the presented theory and experiments cannot be expected at low frequencies where the joint is only a few flexural wavelengths long and also at high frequencies (above coincidence) where radiation dominates the internal loss factor.

4. Vibratory Response of Cantilevered Panel

In subsection 1, we derived an expression shown in Equation (3.4), for the vibratory response of a panel substructure attached to another randomly excited panel structure. We should like to apply this formula to the welded plate configuration shown in Figure 3.10. In terms of the thicknesses h_1 and h_2 of plates 1 and 2 respectively and the coupling and loss factors, the acceleration spectrum ratio is

$$\frac{S_1^a}{S_2^a} = \left(\frac{h_2}{h_1} \right)^2 \frac{\eta_c}{\eta_c + \eta_1} \quad (3.27)$$

For the plates studied, $h_1 = .057''$ and $h_2 = .118''$. The coupling η_c is determined from the measured value of γ given in Figure 3.10 by using Equation (3.26). The substructure damping η_1 was measured with and without applied damping. A comparison of the measured response ratio with the computed values without applied damping on plate 1 is shown in Figure 3.13. A similar comparison is shown with plate 1 (substructure panel) more heavily damped.

Although the agreement achieved is not precise, the values tend to lie within a 3 db range of each other and we would probably regard the calculations as a reasonable engineering estimate of the observed response.

D. REDUCTION OF BEAM-PLATE COUPLING BY NOTCHING BEAM

The beam which was described in Figure 3.2 was notched for the purpose of reducing the plate-beam coupling. The location of the notch and definitions of dimensions are shown in Figure 3.11. Since the reduction of coupling is only effective in reducing the vibration when $\eta_c < \eta_b$, the experiments were run with applied damping on the beam. The octave band results with no notch were shown in Figure 3.4 and are reproduced in Figure 3.12 under the caption $w_s = 1.5''$, $l_s = 0$.

The width of the joining stud is w_s and its length is l_s . The ratio of beam to plate vibration is shown for various values of these dimensions in Figure 3.12. Qualitatively the longer and thinner the stud, the greater is the reduction in vibration. We do notice a resonance effect for the stud $l_s = 0.8"$, $w_s = 0.1"$ at about 6 kc. This corresponds to $kl_s \sim 1$ where k is the wavenumber for flexural waves.

NOTES AND REFERENCES FOR APPENDIX III

1. R. H. Lyon and G. Maidanik, "Power flow between linearly coupled oscillators," J. Acoust. Soc. Am. 34, 623, May, 1962.
2. M. A. Heckl, "Compendium of impedance formulas," Bolt Beranek and Newman Inc., Report No. 774, ONR Contract NONR 2322(00), May, 1961.
3. R. Courant and D. Hilbert, Methoden der Mathematischen Physik, I, (Springer-Verlog, Berlin, 1931), Chapter 6, p. 400.
4. The reverberation time of the structure was measured with an instrument developed by B. G. Watters at Bolt Beranek and Newman Inc. The instrument compares the structural decay to the decay of an RC circuit of known time constant. It is capable of measuring reverberation times as short as 10^{-2} sec. The shortest reverberation time encountered in our experiment was 3×10^{-2} sec.
5. A. E. H. Love, The Mathematical Theory of Elasticity, (Dover Publications, New York, 1944), Chapter XXII.
6. M. Heckl, "Measurements of absorption coefficients on plates," J. Acoust. Soc. Am. 34, 6, 803-808, June, 1962.

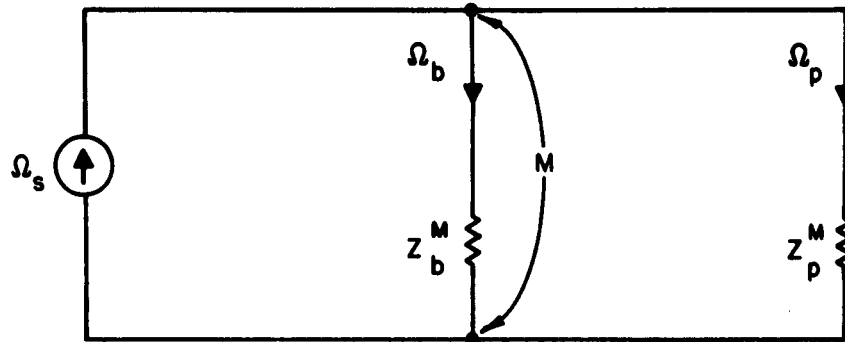


FIG.3.1 ANALOG CIRCUIT FOR THE MOMENT AT THE BEAM-PLATE INTERFACE

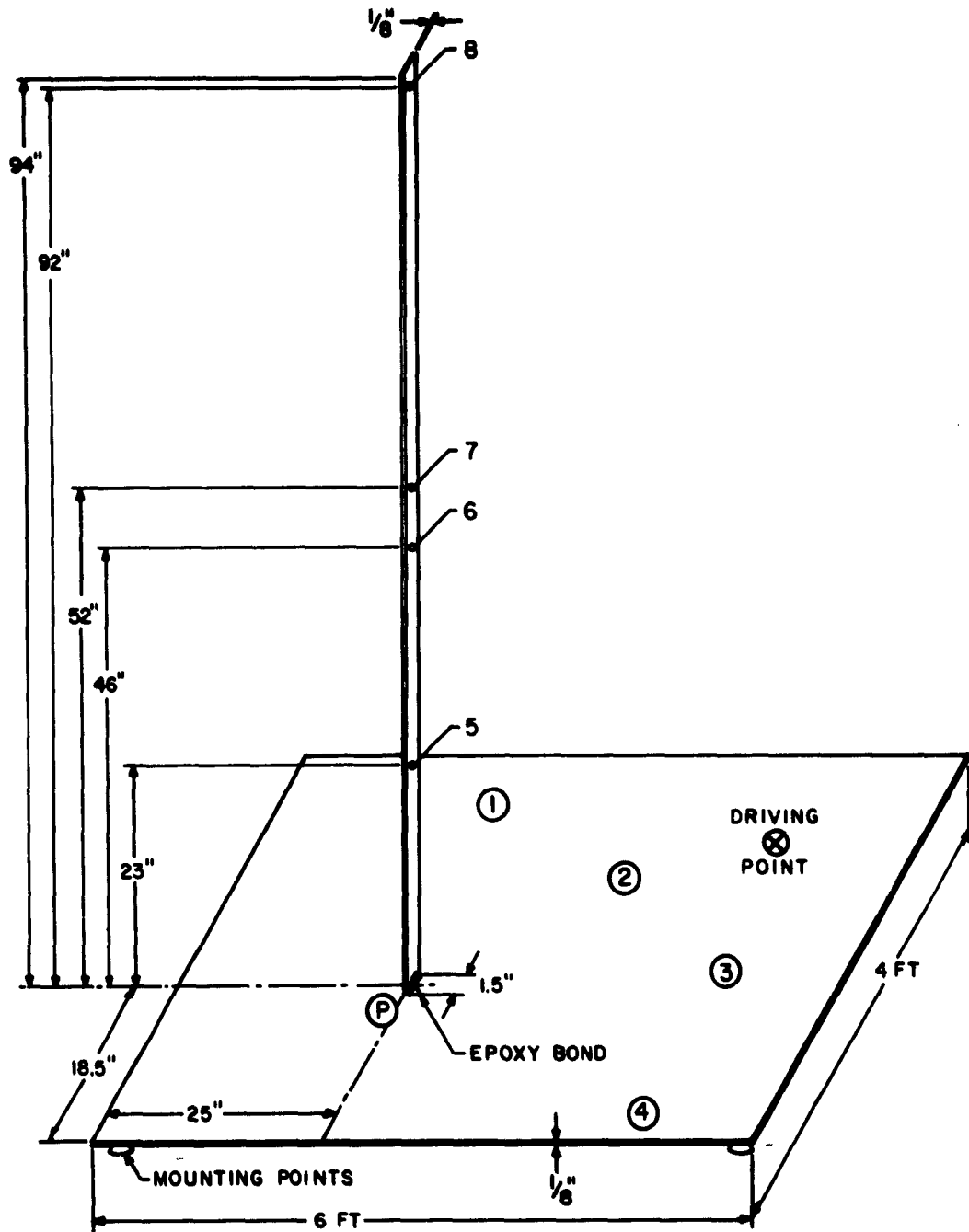


FIG. 3.2 SCHEMATIC DIAGRAM OF BEAM-PLATE SYSTEM

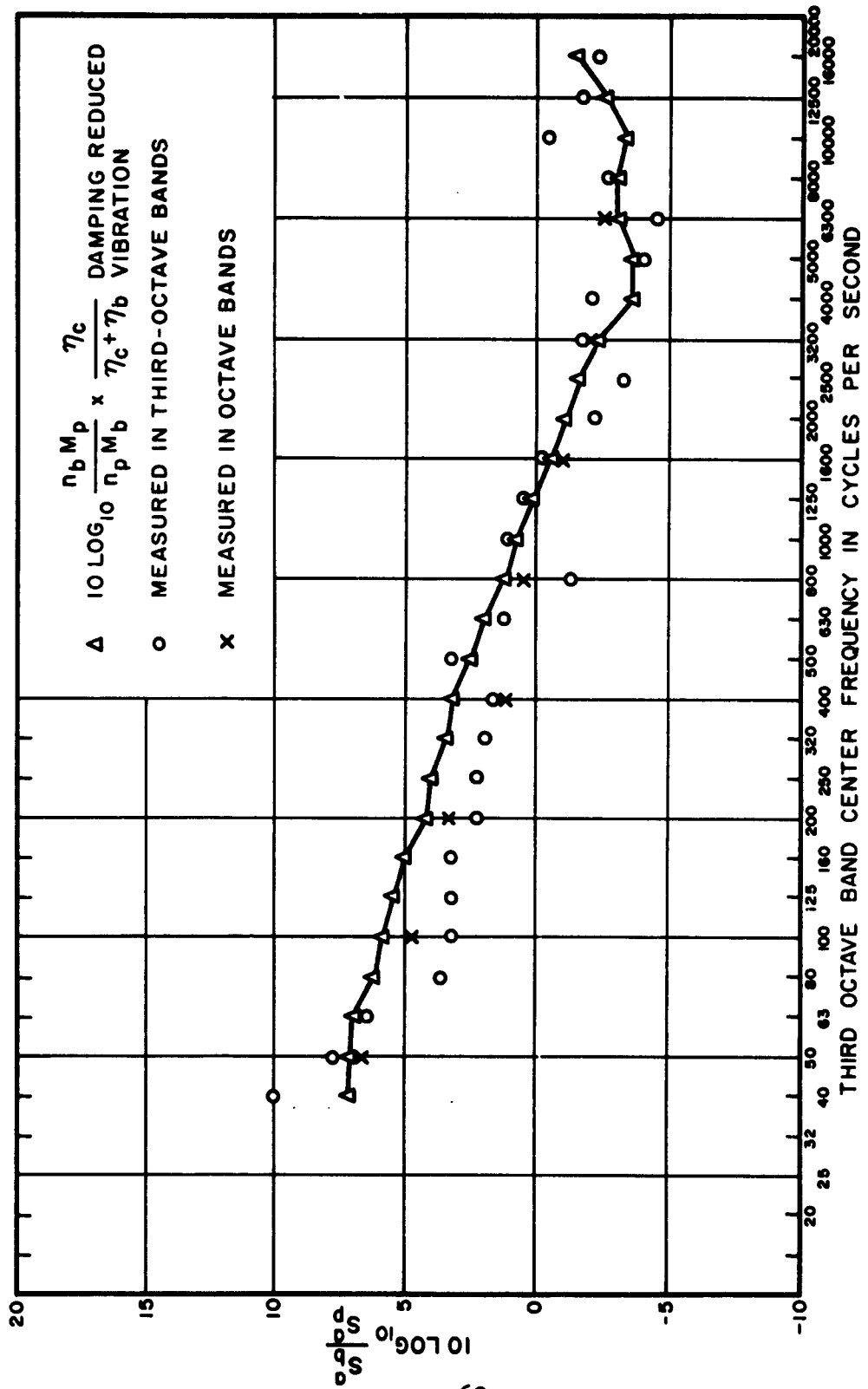


FIG. 3.3 DIRECT AND INDIRECT MEASUREMENTS OF RESPONSE RATIOS WITHOUT APPLIED DAMPING

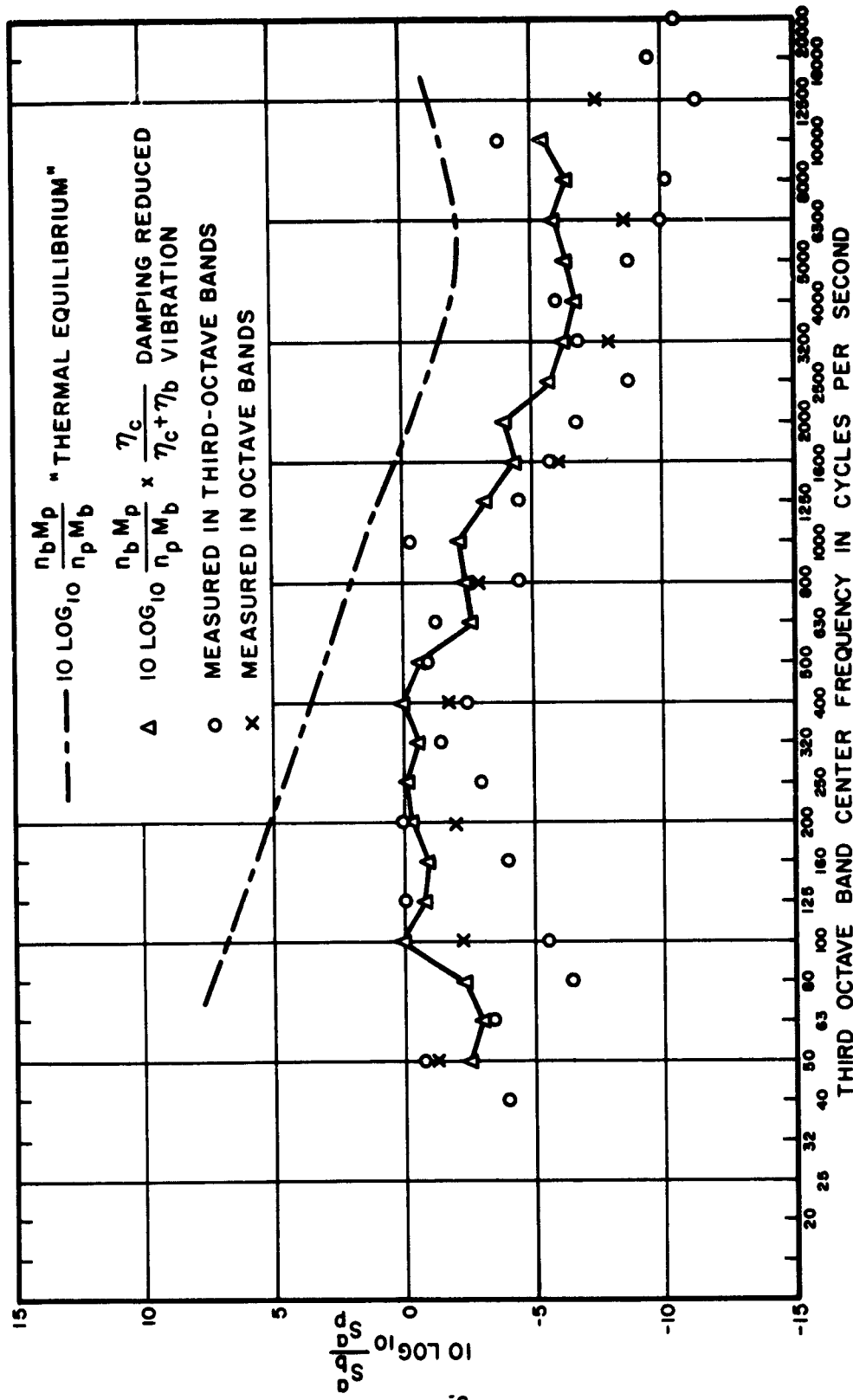
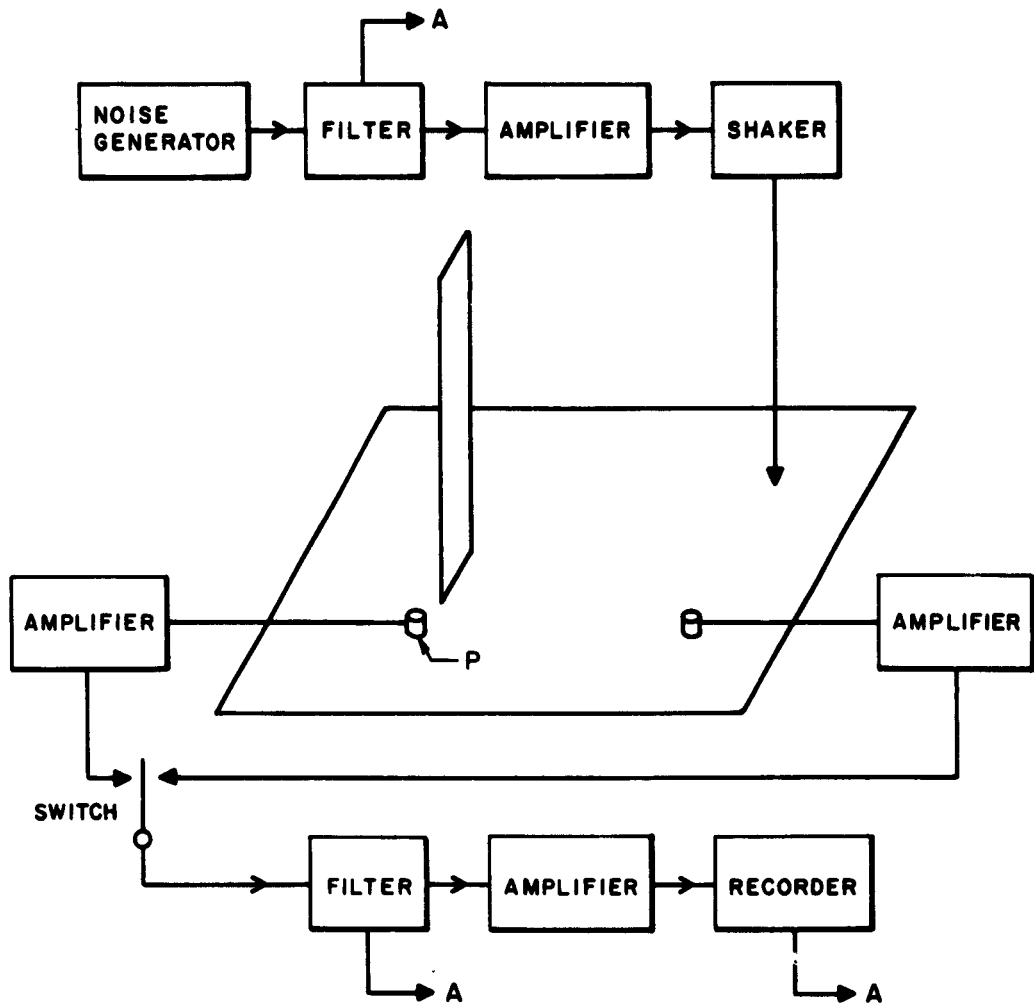


FIG. 3.4 DIRECT AND INDIRECT MEASUREMENTS OF RESPONSE RATIOS WITH APPLIED DAMPING



"A" DENOTES COMMON MECHANICAL DRIVE

FIG. 3.5 EXPERIMENTAL FLOW DIAGRAM FOR DIRECT MEASUREMENT OF S_b^a/S_p^a

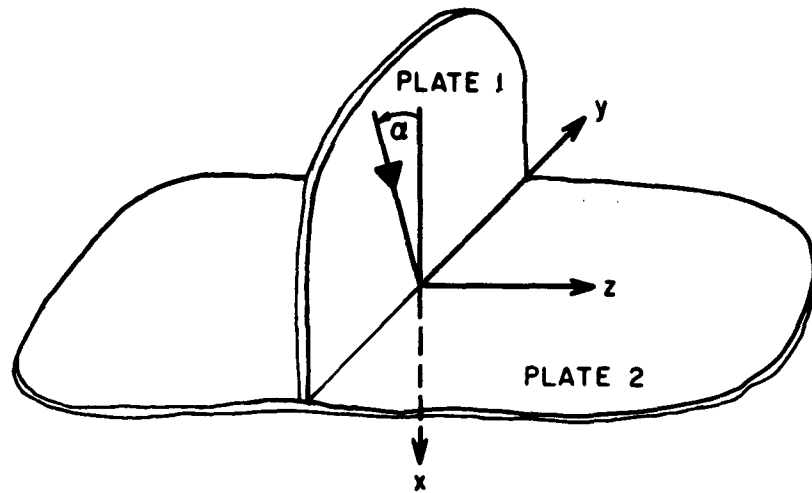


FIG. 3.6 PLATE GEOMETRY

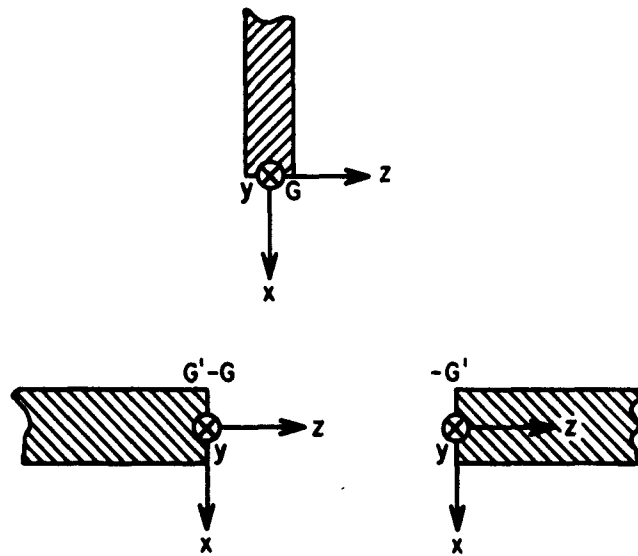


FIG. 3.7 PLATE BOUNDARY CONDITIONS

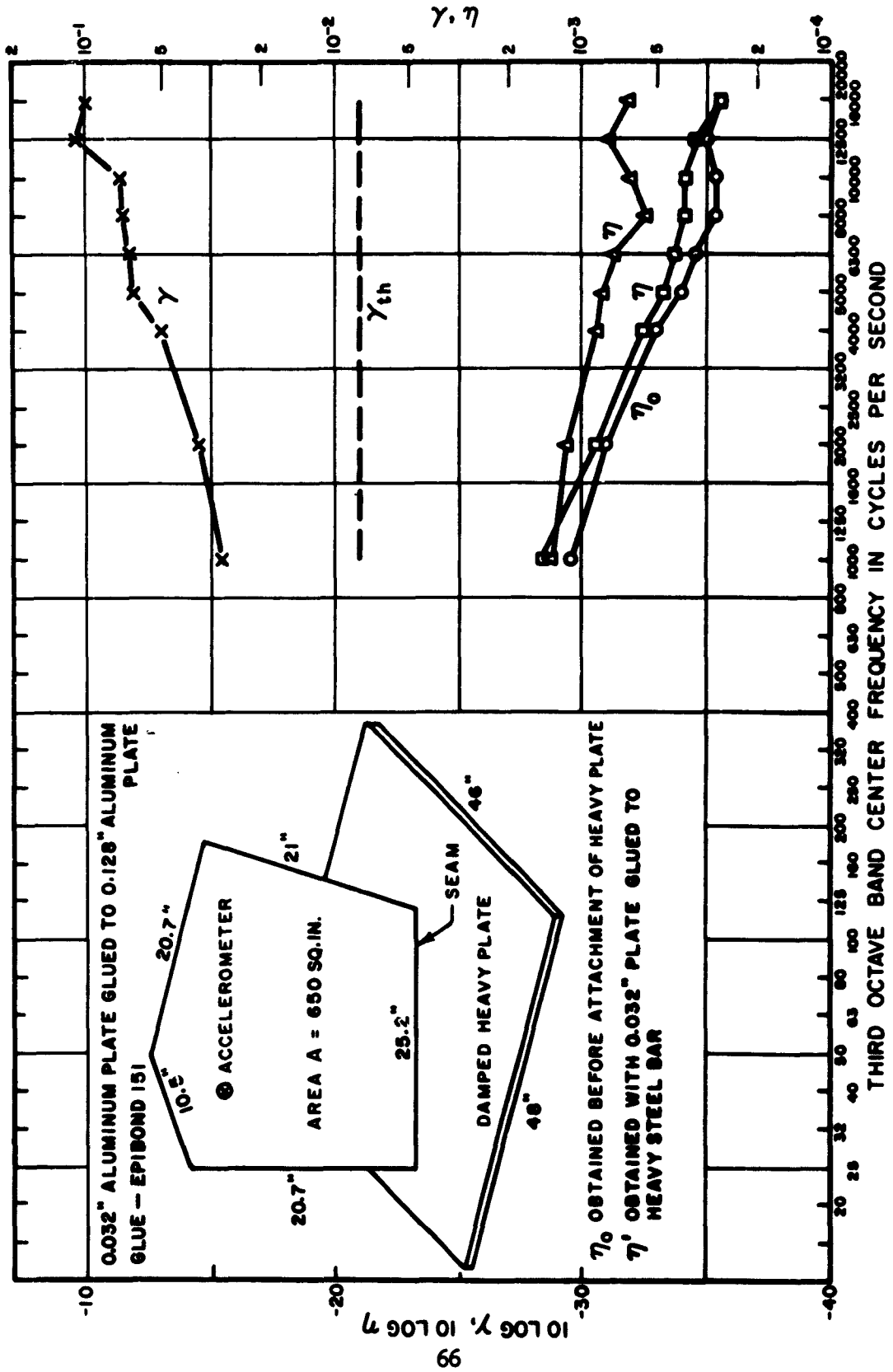


FIG. 3.8 LOSS FACTORS AND ABSORPTION COEFFICIENT OF 0.032" GLUED ALUMINUM PLATE

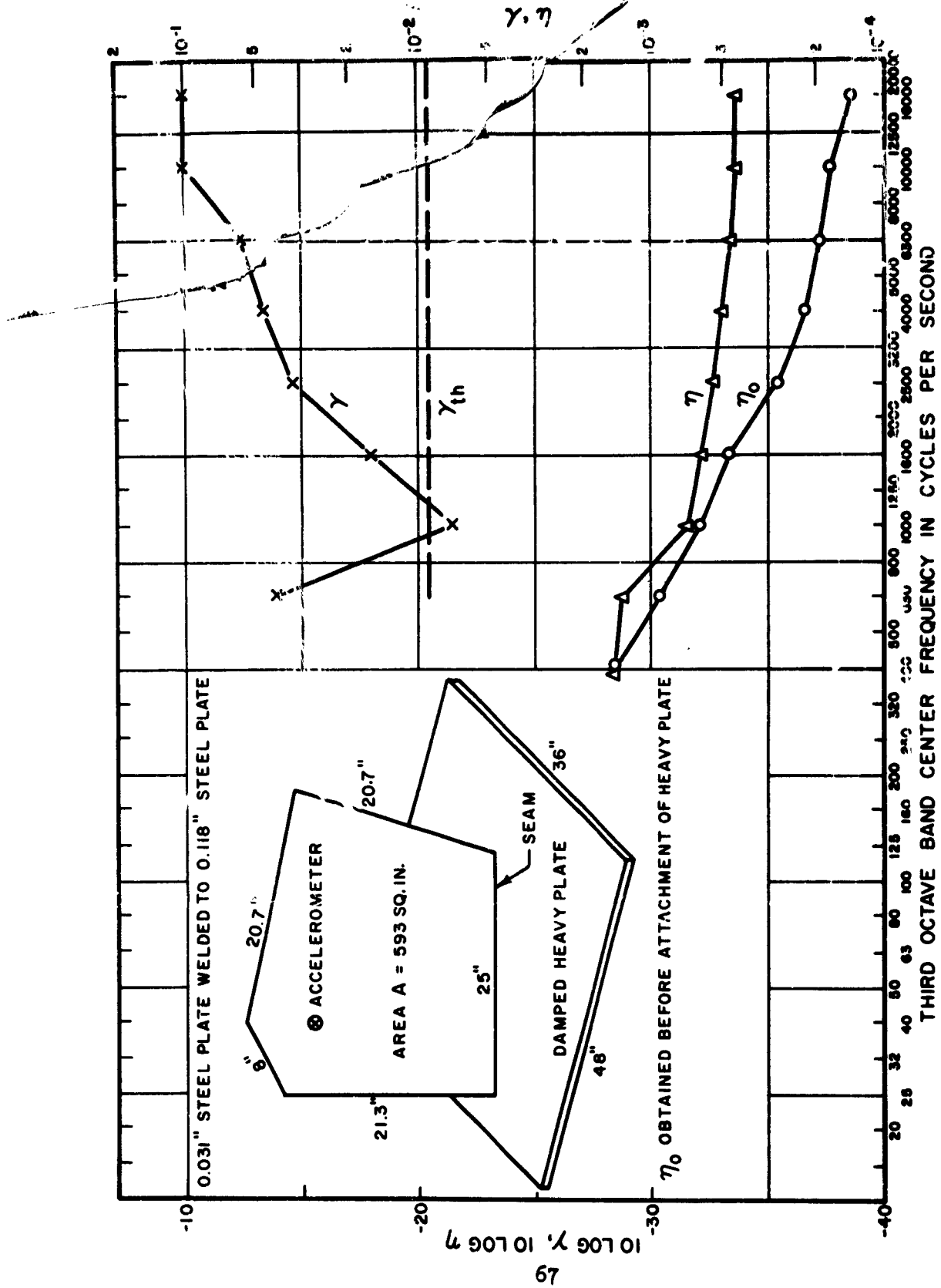


FIG. 3.9 LOSS FACTORS AND ABSORPTION COEFFICIENT OF 0.031" WELDED STEEL PLATE

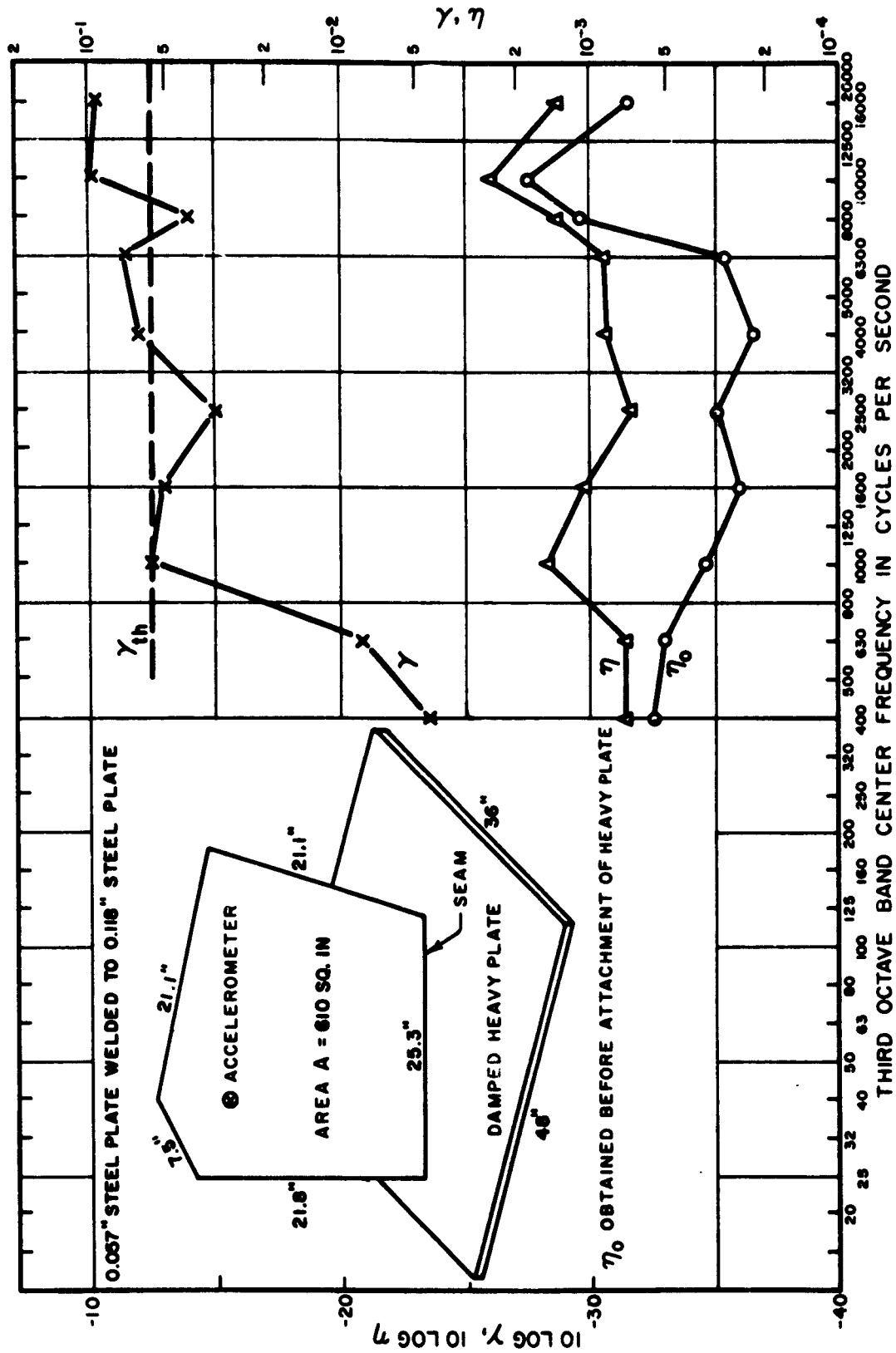


FIG. 3.10 LOSS FACTORS AND ABSORPTION COEFFICIENT OF 0.057" WELDED STEEL PLATE

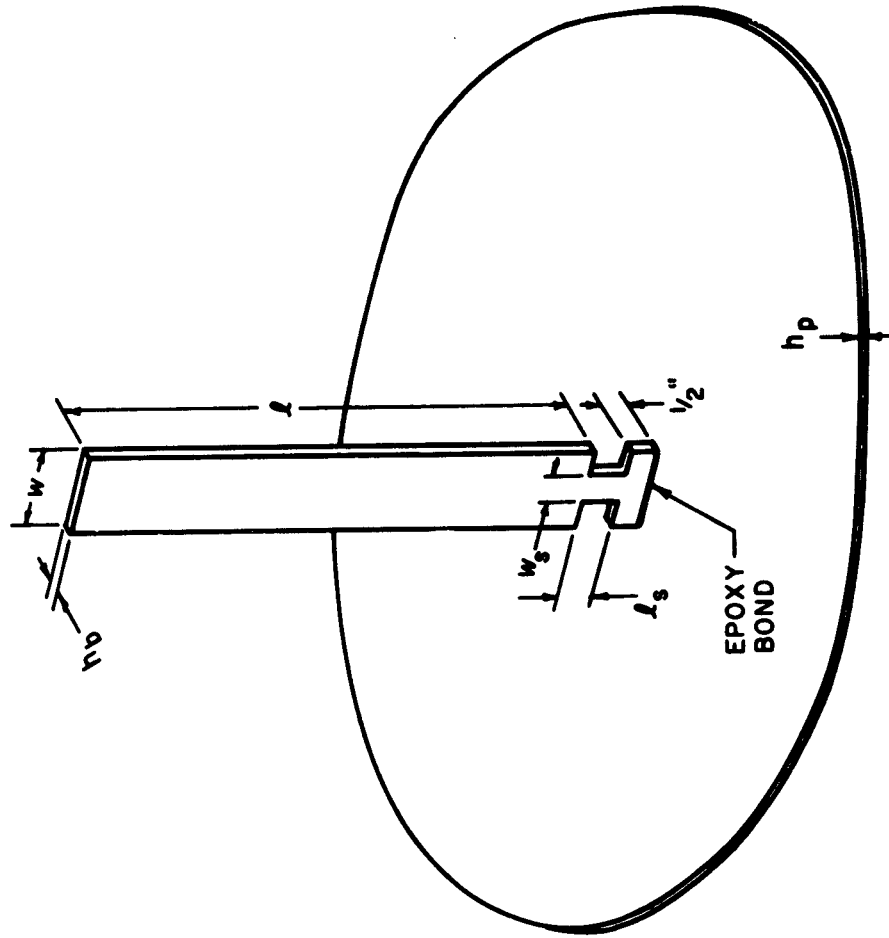


FIG. 3.11 PLATE-BEAM SYSTEM SHOWING THE CUT MADE TO REDUCE THE COUPLING

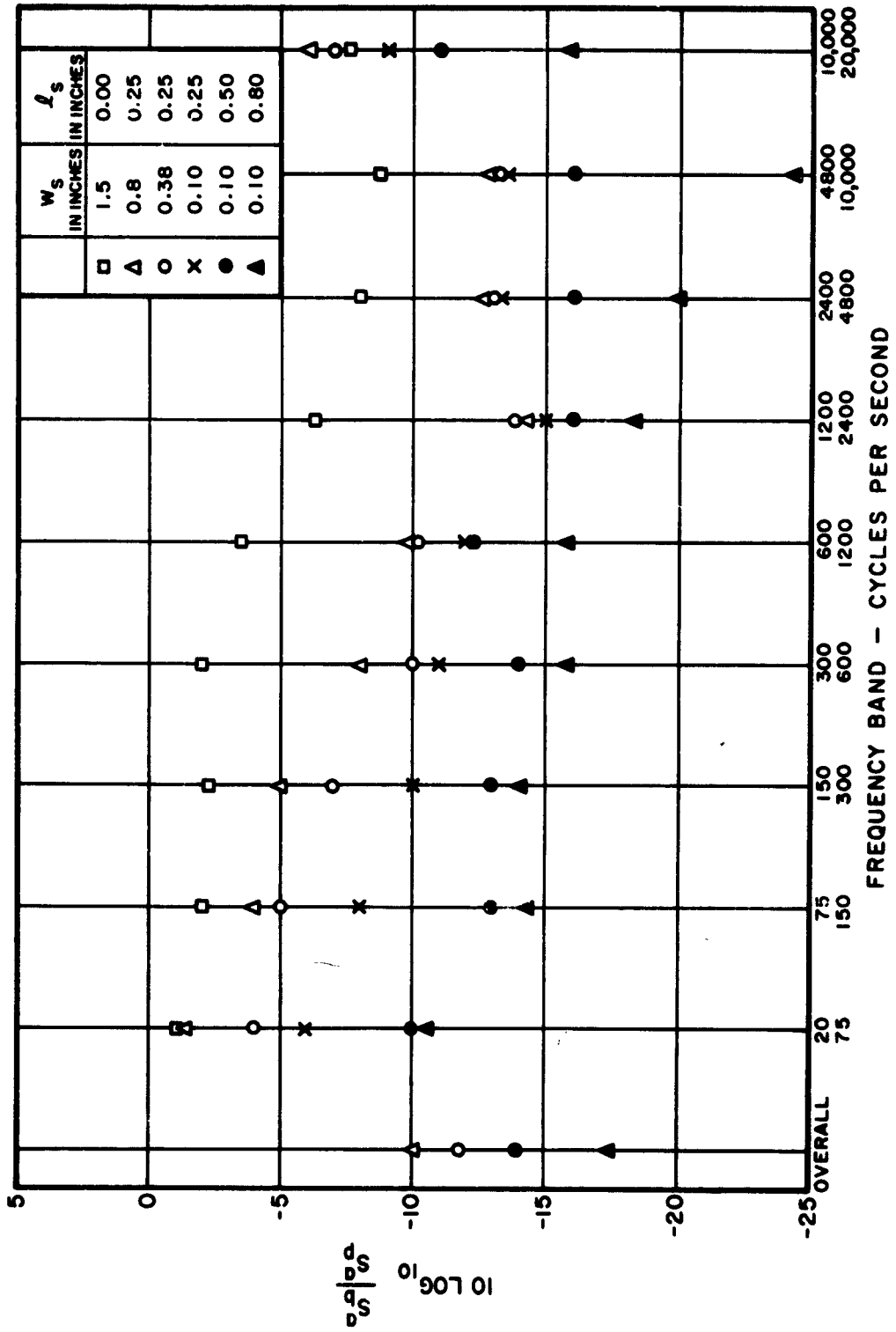


FIG. 3. 12 THE RESPONSE OF A BEAM CANTILEVERED TO FLAT PLATE

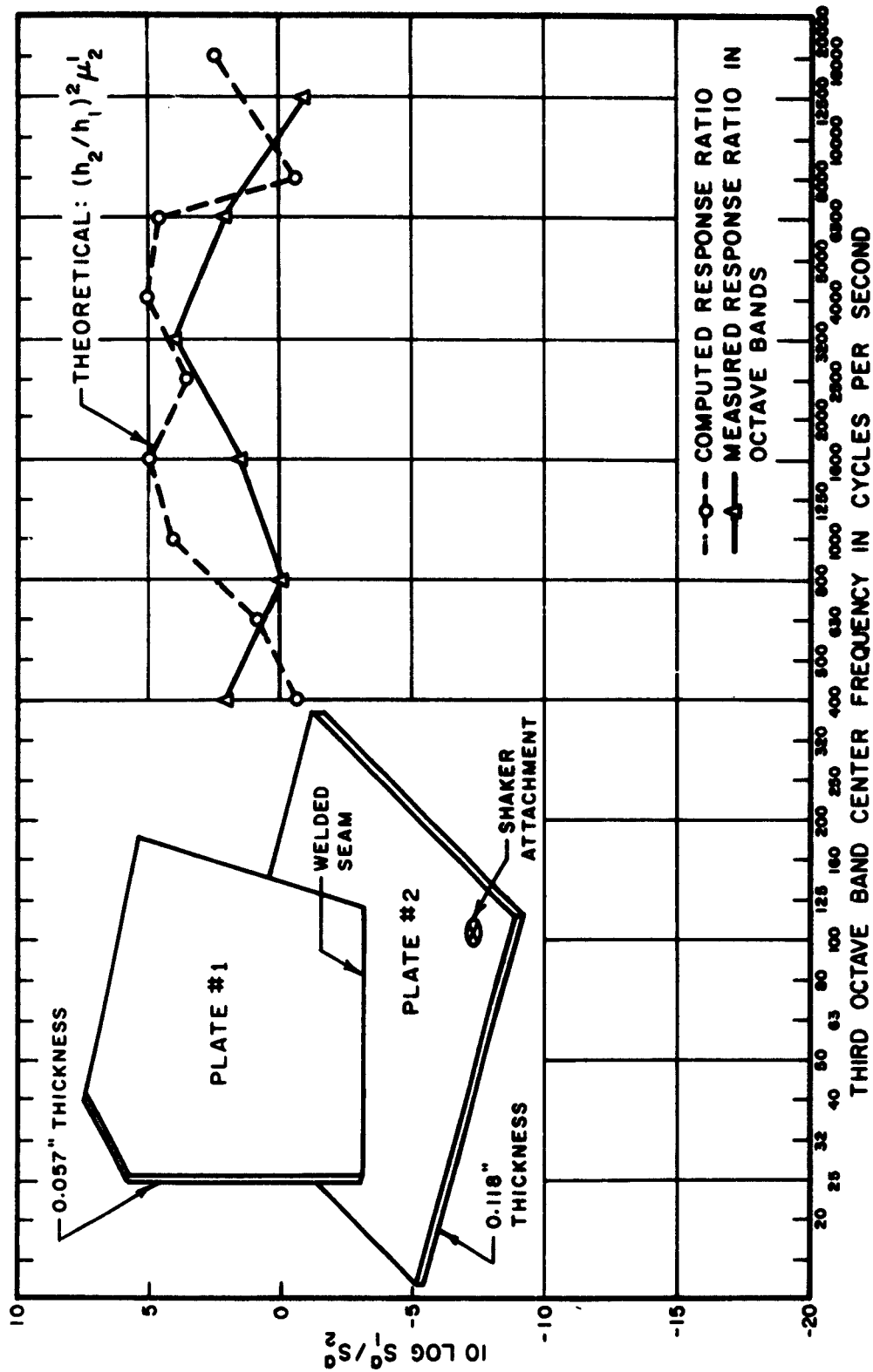


FIG. 3.13 RELATIVE VIBRATION LEVELS OF CONNECTED REVERBERANT PLATES

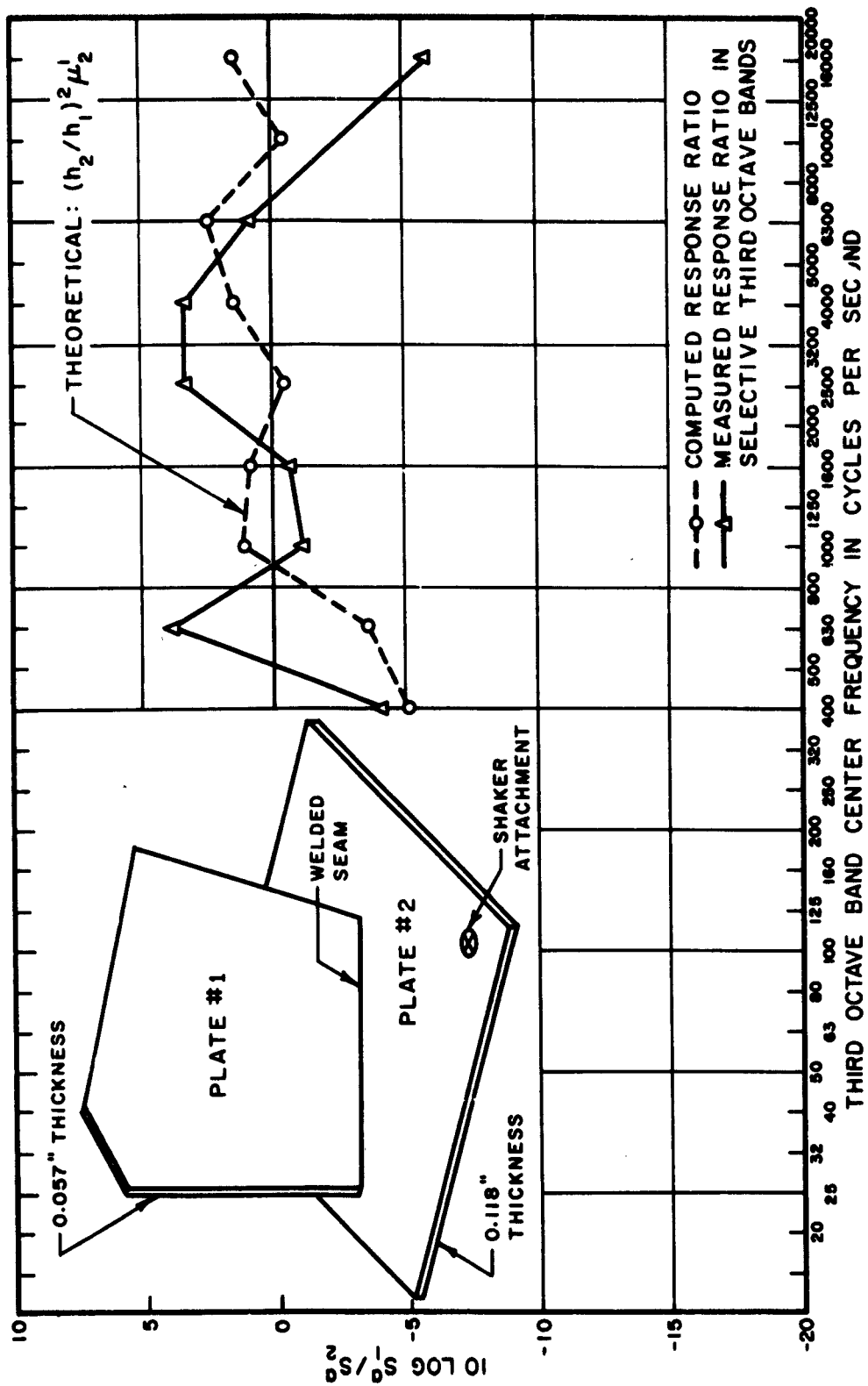


FIG. 3.14 RELATIVE VIBRATION LEVELS OF CONNECTED REVERBERANT PLATES
(PLATE 1 LIGHTLY DAMPED)

Aeronautical Systems Division, Dir/Engineering Test, Environmental Division, Wright-Patterson AFB, Ohio.
Rpt No. ASD-EDR-63-205. RANDOM VIBRATION OF STUDIES OF COUPLED STRUCTURES IN ELECTRONIC REQUIREMENTS. Final report, Apr 63. 72pp. Incl illus., 26 refs.

Unclassified Report
The research has centered on two main categories; the replacement of acoustic excitation by direct mechanical excitation of structures and the response of substructures which are tied to a randomly vibrating structure. Studies are included on the power transferred to a plate by a shaker, the

(over)

Variation in vibratory response at various positions and frequency bands, and the energy sharing between randomly excited structures which have mechanical connections. Plans for further research are also included.

1. Random vibration and acoustical equivalence of coupled structures
1. AFSC Project 1309.
Task 130904

II. Contract No.
AF 33(657)-9118
III. Bolt Barnack and Newman Inc., Cambridge, Mass.
IV. Richard H. Lyon et al
V. Aval fr CES
VI. In AFSA collection

Aeronautical Systems Division, Dir/Engineering Test, Environmental Division, Wright-Patterson AFB, Ohio.

Rpt No. ASD-EDR-63-205. RANDOM VIBRATION OF STUDIES OF COUPLED STRUCTURES IN ELECTRONIC REQUIREMENTS. Final report, Apr 63. 72pp. Incl illus., 26 refs.

Unclassified Report
The research has centered on two main categories; the replacement of acoustic excitation by direct mechanical excitation of structures and the response of substructures which are tied to a randomly vibrating structure. Studies are included on the power transferred to a plate by a shaker, the

(over)

variation in vibratory response at various positions and frequency bands, and the energy sharing between randomly excited structures which have mechanical connections. Plans for further research are also included.

1. Random vibration and acoustical equivalence of coupled structures
I. AFSC Project 1309.
Task 130904

II. Contract No.
AF 33(657)-9118
III. Bolt Barnack and Newman Inc., Cambridge, Mass.
IV. Richard H. Lyon et al
V. Aval fr CES
VI. In AFSA collection